Check for updates

Multi-functional metal–organic frameworks for detection and removal of water pollutions

Yang Li,[a] Jiandong Pang (ID) *[ab] and Xian-He Bu (ID) *[abc]

Water pollutions have caused serious threats to the aquatic environment and human health, it is of great significance to monitor and control their contents in water. Compared with the traditional single treatment method, multiple treatment can simultaneously realize detection and removal of water pollutions on one material, which brings convenience and promotes comprehensive treatment for water remediation. Metal–organic frameworks (MOFs) are versatile porous materials that hold huge potential in wastewater treatments. This feature article reviews the recent advances in MOFs for multifunctional water treatment. First, strategies to design the sensing, removal and degradation functions onto MOFs are introduced. Then, the sensing, removal and degradation effects on various inorganic and organic water pollutions based on multifunctional MOF materials are summarized, and the interaction mechanisms are discussed in detail. Finally, the current challenges and the future research trends on MOF materials for wastewater treatment are discussed as well.

1. Introduction

In the past decades, the humanity knowledge and transformation ability of nature further strengthen along with the swift and violent development of science and technology. However, rapid industrialization, accelerated urbanization, surging exploitation of resources, direct discard of wastes and so forth caused by human activities have placed an enormous burden on the environment, especially on water resources.[1] As a result, a variety of contaminants have lowered the water quality extensively and brought about water pollution. Generally, Water pollution consist of miscellaneous inorganic and organic substances such as halide ion, heavy metals, radionuclides, oxysalt, synthetic dyes, herbicides, pesticides, persistent organic pollutants (POPs), endocrine disrupting chemicals (EDCs), pharmaceuticals and personal care products (PPCPs) and emerging organic contaminants (EOCs), *etc.*[2–9] These hazardous contaminants are relatively stable in water and can possess carcinogenic, teratogenic and mutagenic effects, leading to adverse impact to both environment and human health.[10,11] It is of great significance to detect and remove water pollutions effectively for the sake of preventing their repercussions.

Up to now, A variety of wastewater treatments have been carried out for the remediation of aqueous environment, most of which can be summarized as the following strategies: sensing, removal and degradation. Sensing refers to methods for the determination of water pollutions with high sensitivity and selectivity, among which electrochemical, optical and electronic signals are common outputs.[12] Numerous materials, for instance, small molecules, polymeric materials, nanomaterials and porous materials are exploited for various water contaminants detecting with low limit of detection and high selectivity.[13–15] Removal is the basic function in water treatment to eliminate pollutions from aqueous environment *via* multifarious functional materials. It contains a number of techniques *viz.* coagulation, membrane filtration, chemical precipitation, ion exchange, electrodialysis, flocculation and adsorption.[16–19] Adsorption is one of the most widely used approaches among them, due to the ease of operation, high efficiency, relatively low cost and reusability. Adsorbents play a crucial role in this method and various adsorbents, namely activated carbons, zeolites, graphene-based materials, clay minerals, resins and porous materials have been developed for eliminating all kinds of water pollutions with large adsorption capacity and high removal efficiency.[20–25] Degradation is an option for water treatment by decomposing organic pollutions or oxidizing/reducing metal ions to a low toxicity state. Diversified methods, *e.g.*, photocatalysis, electrocatalysis, Fenton reaction, ozonation and chlorination are widely explored for water pollution detoxication.[26–30] Semiconductor materials like TiO_2, WO_3, CuS, CdS, ZnO and Fe_2O_3, *etc.*, are typical catalytically active substances. In the last decades,

[a] *School of Materials Science and Engineering, National Institute for Advanced Materials, TKL of Metal and Molecule-Based Material Chemistry, Nankai University, Tianjin 300350, P. R. China. E-mail: buxh@nankai.edu.cn, jdpang@nankai.edu.cn*

[b] *Haihe Laboratory of Sustainable Chemical Transformations, Tianjin, 300192, P. R. China*

[c] *State Key Laboratory of Elemento–Organic Chemistry, College of Chemistry, Nankai University, Tianjin 300071, P. R. China*

organic materials, for instance, graphene, carbon nanotube and g-C$_3$N$_4$ and inorganic–organic hybrid materials such as metal–organic frameworks are burgeoning materials that reveal great potential for wastewater degradation.[31–34]

Impressing progress has been made for water pollution control. However, most research focus on realizing one function of sensing, removal or degradation. As the research and practice is continually comprehensive and in-depth, single-function treatment of wastewater has its limitation. For example, sensing probes commonly lack sufficient adsorption capacity, and additional adsorption material is needed to remove the pollutions after their detection; the concentrated adsorbed pollutions on adsorbent need to be carefully treated in order to avoid secondary pollution to the environment;[35] Traditional catalyst, *e.g.*, TiO$_2$ often suffers from low surface area and shows low abundance catalytic sites toward analytes, thus displaying reduced catalytic efficiency.[36] Integration of different functions to a single system, *viz.* construction of multifunctional materials can combine their respective advantages and implement multi-purpose applications, gradually developed in energy, biomedicine, materials science, *etc.*[37–39] For water pollution treatment, exploiting materials with more than one function of sensing, removal or degradation to the specific target can help simultaneously detect and control pollutions in water, which is a promising way for comprehensive treatment of water pollutions. Nevertheless, this kind of strategy requires higher designability and versatility of materials, for which advanced materials are desired.

Metal–organic frameworks (MOFs) represent a class of porous inorganic–organic hybrid materials coming forth in the last decades that are synthesized through the assembly of secondary building units (SBUs), *viz.*, organic linkers and metal cations/clusters *via* coordination bond.[40] The crystalline structure, high porosity, high surface area, atomic-level precision design and multiplicate chemical properties enable MOFs to be utilized in copious applications involving energy storage, separation, bioimaging, catalysis, sensing, and so on.[41–44] MOFs also demonstrate huge potential in water treatment field and a number of articles

and reviews are reported.[45–47] However, most studies mainly focus on one function, namely, sensing, removal or degradation for water pollution disposal. Synthesizing functional MOFs with multiple processing to a certain pollutant is of great significance to detect and eliminate water pollutions on one platform. Such integrated water treatment platform puts forward elegant design request for MOF-based materials.

In this feature article, we investigate the design strategy to accomplish the sensing, removal and degradation functions in MOFs and summarize the near-term advances in multifunctional MOFs for water pollution treatment. Furthermore, the current challenges for the multiple treatment of water pollution are discussed, and the outlook on strategies for further developments are recommended (Scheme 1).

2. MOFs design for water pollution treatment

MOFs have been explored for water pollution treatment in the past 15 years, while the first MOF for sensing was reported (Cu^{2+} ion) in aqueous solution in 2010,[48] the first MOF for the removal of methyl orange (dye) from water in 2010[49] and the first MOF for degradation of phenol (industrial product) in 2007.[50] Since then, MOFs are vastly developed as wastewater treatment materials duo to the following features: (I) high surface area, facilitating adsorption process;[51] (II) accurate design at atomic level, where sensing/catalytic sites towards the analytes can be precisely embedded into the structure;[52] (III) accessible and functionalized pores, where host–guest inter-actions with selectivity may occur;[53] (IV) crystalline feature, which is convenient to explore the mechanism;[54] (V) stability, with which a number of water stable MOFs can be achieved for water treatment;[55] (VI) processibility, where MOFs can be manufactured to various devices.[56] In recent years, MOFs with multifunction for water pollution treatment have been reported. MOFs are ideal materials for water pollution treatment and by virtue of their atom level accurate design and intrinsic porosity, specific interaction towards analytes can be realized. On the basis of adsorption of targets on MOFs, sensing and degradation functions can be conducted on the same material by rational and elegant design of the monomers. Design strategy of MOFs for sensing, removal and degradation of water pollutions are discussed below.

2.1 MOFs for sensing

Sensing is a sensitive way to detect water pollutions with selectivity. MOFs are good candidates for water pollution sensing, since the constitutional units (ligand, metal ions or clusters) of MOFs have greatly variability and tunability that may generate electro/optical signals change after the interactions with analytes.[57] Besides, the intrinsic porosity of MOFs plays an important role in sensing the targets. On one hand, the pores allow the analytes to enter into the framework and confine their motion to some extent, facilitating the interactions between MOFs and analytes.[58] On the other hand, the pores can be elegantly tuned both in size and
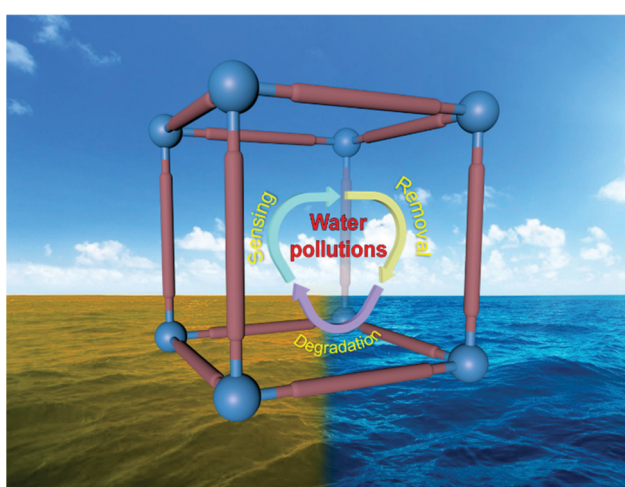
Scheme 1 Schematic representation for the multiple treatment of water pollutants on MOFs.

chemical environment *via* the regulation of MOFs construction through bottom-up or post-modification strategy.[59,60] As a result, a variety of MOFs are synthesized by rationally designing metal ions/clusters and organic ligands for sensing water pollution.[61]

2.2 MOFs for removal

Removal of pollutions from aqueous solution is a particularly important mode in water treatment. MOFs exhibit unique characteristics in water pollution removal as such materials combine porosity, crystallinity and functionality. Porosity can help accommodate more analytes and increase removal efficiency. It is worth noting that pore size and surface area of MOFs can be tuned by changing the connectivity and structure of the organic ligand.[62] MOFs with suitable pores can be synthesized to meet the removal requirements of pollutions with different size. Crystallinity enables MOFs to be determined at atomic precision, and the interactions with the targets can be revealed. A better understanding of the removal mechanism is hence given.[63] Functionality is a fascinating feature in MOFs, where the diversity of organic linkers can be applied to the MOFs structure and brings about binding sites to the analytes. As a result, various interactions, for example, electrostatic interaction, hydrogen bonding, π–π interaction, acid–base interaction and hydrophobic interaction can be induced to the framework through organic ligands design to enhance the adsorption ability of the analytes in water. [54] Besides organic linkers, inorganic metals can also contact with the analytes *via* the interactions between their uncoordinated orbitals and the heteroatoms (O, N, S, *etc.*) of the adsorbates.[64]

2.3 MOFs for degradation

Degradation of water pollutions is a considerable approach as such process can transform pollutions to less toxic or nontoxic form. MOFs exhibit satisfactory performance in the degradation of water pollutions as their porosity can offer a suitable space for the chemical reactions to take place. Besides, MOFs consist of metal/metal clusters and organic ligands, both of which can be used as catalytic sites *via* meticulous design.[65,66] Through the functional adjustment of organic ligands, *e.g.*, introducing –NH$_2$, –OH, –SH, halogen or heteroatom, the bandgap of MOFs can be tuned and a better catalytic performance can be acquired.[67,68] In addition, doping is another efficient strategy to obtain effective catalyst for water pollution treatment based on MOFs. Noble metals like Au, Pd and Pt,[69,70] metal semiconductors such as TiO$_2$[71] and ZnO[72] and carbon materials, for example, graphene oxide[73] and g-C$_3$N$_4$[74] are integrated with MOFs to enhance the catalytic performance towards water pollution.

Adsorption plays a critical role in water pollution treatment as such process enables analytes to separate from aqueous environment and attach to the adsorbent, after which the sensing or catalysis procedure can occur efficiently. The high surface area and porosity of MOFs make it good candidates to perform adsorption process towards analytes and promising platform to carry out removal, sensing and degradation functions. Removal process caused by adsorption is a fundamental function in water pollution treatment, however, analytes absorbed on

MOFs may not necessarily lead to sensing or degradation response. By judicious choice of metal type, connectivity, ligand size, structure and function, multi-functional water pollution treatment materials based on MOFs can be accessed. In addition, removal, sensing and degradation of the same target help to monitor and control the specific pollution in water simultaneously, and is mainly discussed in this feature article.

3. Multifunctional MOFs for water pollution treatment

Scientists have synthesized a number of MOFs for wastewater treatment and achieved decent progress, however, pursuing MOFs with multiple-modality in water pollution treatment is far from over. Considering the diversity of water pollutions, the realization of sensing, removal and degradation of a specific contaminant on MOFs/MOF composites, and the exploitation of various functional MOFs for multiple treatment of different analytes, is expected (Fig. 1).

3.1. MOFs for multiple treatments of inorganic pollutions in water

Water pollutions have a diversity of sources and are numerous in variety.[75–77] According to the constitution, water pollutions can be divided to organic and inorganic contaminants. Inorganic pollutions mainly include heavy metals, halide ion, oxyanions and radioactive elements.[78,79] Adsorptive removal and sensing are frequently-used methods to detect and control inorganic water pollutions. As most inorganic pollutions are hard to degrade, some catalytic redox reactions can make the valence of metal transform to a low-toxic state, providing another way for inorganic pollution treatment.[80,81]

3.1.1. Mercury treatment. Mercury is a considerable toxic heavy metal and is harmful for human body by influencing their nervous system and endocrine system, resulting in several diseases like Minamata disease.[82,83] Removal and sensing of mercury ion simultaneously is of great significance and is one of the most studied cations on MOFs. Due to the strong affinity of mercury to the soft center, S, introduction of sulfur into MOFs is an effective and efficient means. Li and co-workers successfully designed and synthesized an isoreticular series of luminescent MOFs (LMOF-261, -262, -263) by incorporating a strongly emissive molecular fluorophore and colinkers into Zn-based structures (Fig. 2).[84] Thereinto, LMOF-263 displayed impressive water
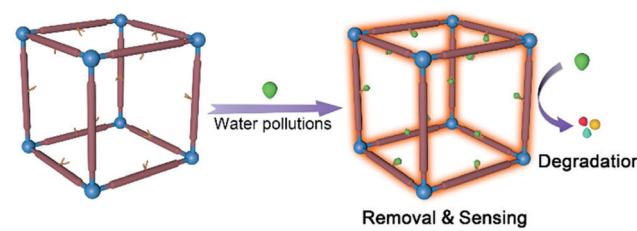
Fig. 1 Illustration for the sensing, removal and degradation functions realized on multifunctional MOFs for water pollutions treatment.
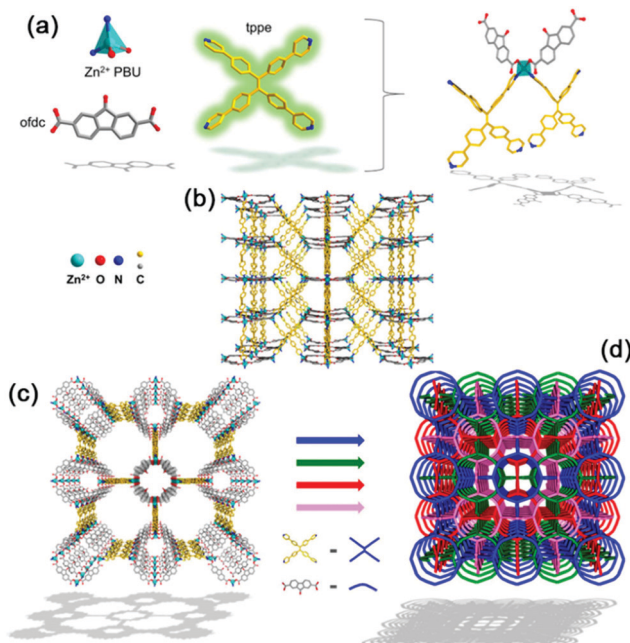
Fig. 2 Schematic illustration of the structure of LMOF-261 for adsorption and sensing of Hg ion. Reproduced from ref. 84 with permission from American Chemical Society, copyright 2016.

stability, high porosity and strong luminescence. Such MOF can response to mercury ion by monitoring the photoluminescence change at a parts per billion level (3.3 ppb) and showed high selectivity towards light metals. In addition, LMOF-263 demonstrated a maximum Hg^{2+} adsorption capacity of 380 mg g^{-1} and showed a fast adsorption process with 99.1% Hg^{2+} ion removing within 30 min. Interaction mechanism revealed that sulfur atom within sulfone group in LMOF-263 formed weak π-bonds with the surrounding oxygen, increasing the soft base character of the sulfone. Soft acids such as mercury can have a higher affinity to soft base forming within LMOF-263 according to the HSAB Pearson acid–base concept.

Ligand exchange is also an elegant approach to acquire functional MOFs.[85] In a study by Wang and co-workers, the solvent-assisted ligand exchange approach was conducted to construct a mixed-ligand NH_2-UiO66-SH (NSU66) via introducing the thiol containing ligands to NH_2-UiO-66.[86] The obtained NSU66 displayed a large adsorption capacity of 265.29 mg g^{-1} and a removal rate within 60 min together with qualified selectivity. NSU66 showed a fluorescence quenching effect towards Hg^{2+} with a low detection limit of 3.50×10^{-2} μM and a wide linear range of 1.00–99.7 μM. NSU66 also demonstrated high specificity and strong anti-interference capability during the sensing process. Compared with the NH_2-UiO-66, NSU66 showed a significant enhancement in both sensing and adsorption ability, which benefits from the interactions between the incorporated thiol groups and Hg^{2+}. The photo-induced electron transfer (PET) mechanism was proposed to explain the sensing process. Considering the good stability in water and recyclability, such MOFs can serve as multifunctional platform for sensing and removal of Hg^{2+} ion. In another work by the same group, a

series of classic luminescence MOFs were synthesized based on the same organic ligand, NH_2-H_2BDC, and different central metals (Ti^{4+}, Fe^{3+}, Cr^{3+}, Zr^{4+} and Al^{3+}).[87] Among these MOFs, NH_2-MIL-53(Al) displayed good sensing ability towards Hg^{2+} with the response range of 1–17.3 μM, low detection limit of 0.15 μM, good selectivity and wide pH adaptation of 4.0–10.0. Meanwhile, the NH_2-MIL-53(Al) showed an adsorption capacity of 153.85 mg g^{-1} and an uptake kinetic within 60 min. NH_2-MIL-53(Al) demonstrated excellent stability due to the formation of strong coordination bonds between high oxidation state aluminium (Al^{3+}) and organic carboxylate ligands. The satisfactory reusability endowed the NH_2-MIL-53(Al) a promising application prospect for sensing and removal of Hg^{2+} simultaneously in aqueous solution.

Apart from the interaction between the sulphur and mercury, other heteroatoms such as nitrogen and oxygen can also have interactions with Hg^{2+}.[13] Morsali and co-workers introduced S linker which has a malonamide functional group into the Cu-based MOFs to form TMU-46S, -47S and -48S, respectively, via a solvent-assisted ligand exchange (SALE) method.[88] The exchanged MOFs showed a large adsorption capacity of 714 mg g^{-1} towards Hg^{2+} and a limit of detection of 0.1 ppm with the quenching constants (K_{sv}) of 186 087 M^{-1}, and the performance is superior to the original MOFs. The synergistic effects of both hydrophilic chelating malonamide and acylamide functional groups contributed a lot in recognizing mercury ion through theoretical calculations. The research represented an effective way to develop multi-functional MOFs in mercury ion treatment.

Visual monitoring is a direct and convenient method to detect mercury ions.[89] In a research work by Roy's group, a Ni-based MOF was synthesized using an organic ligand that had the uncoordinated sulphur atom.[90] The constructed MOFs had uncoordinated sulphur sites and can form strong bond with mercury due to the soft center of S. The Ni-MOF had a large Hg adsorption capacity of 713 mg g^{-1} in aqueous environment. The colour of the MOF changed from green to grey, thus giving a visual detection of Hg. A number of experiment data and theoretical studies revealed that Hg formed coordinate bonds with S atoms of the SCN$^-$ group. However, one drawback of this system is that the colour change of this MOFs is irreversible and limits its practical use in aqueous solution.

In another research by El-Sewify's group, a novel Al-MOF was synthesized with high surface area to support it as a microporous substrate for further embedding a thioketone derivative chromophore.[91] The thioketone Al-MOF monitors (TAM) were employed through immobilization of chromophore on Al-MOFs' surface. The TAM system had a colour change from yellow to green when contacted with Hg^{2+} ion in water, and the phenomenon can be seen clearly by the naked eye within a few seconds. The sensitivity of TAM to Hg^{2+} can reach 0.8 ppb, which is lower than the WHO permissible drinking water limits. In addition, a very large adsorption capacity of 1110 mg g^{-1} was obtained by TAM in aqueous environment. What is more important is that TAM could be reused several times without losing the sensing and removal ability. The fabricated

TAM was used to sense and remove Hg^{2+} in well water samples and achieve good effects, exhibiting great potential for multi-treatment for Hg^{2+} ion in water.

Electrochemical detection is a sensitive sensing method apart from optical approach.[92] Wang *et al.* reported a mercaptan functionalized MOFs (Zr-DMBD MOFs) by coordination between Zr(IV) and 2,5-dimercaptoterephthalic acid.[93] The MOFs was then combined with kenaf stem-derived carbon (3D-KSC) to form a nanocomposite for electrochemical sensing and removal of Hg(II) simultaneously. The Zr-DMBD MOFs showed the adsorption capacity of 171.5 mg g^{-1}, whereas the Zr-DMBD MOFs/3D-KSC displayed decreased adsorption capacity of 19.3 mg g^{-1}, mainly due to the poor adsorption ability of 3D-KSC towards Hg ion. Zr-DMBD MOFs/3D-KSC demonstrated that the sensitivity of Hg^{2+} was 324.58 μA μM^{-1} cm^{-2}, the linear range was 0.25–3.5 μM and the limit of detection was 0.05 μM. The porous Zr-DMBD MOFs can disperse uniformly on microporous 3D-KSC and offered a great deal of mercaptan groups to enrich Hg^{2+} on the electrode. The Zr-DMBD MOFs/3D-KSC materials showed excellent anti-interference performance, good stability and satisfactory reusability. The S atoms of mercaptan groups on MOFs facilitate the binding process towards Hg ion. The 3D-KSC displayed macroporous structure and high porosity, and Zr-DMBD MOFs were able to grew uniformly on its surface. The mass transfer was thus enhanced and the preconcentration process of Hg ion was accelerated. Furthermore, the Zr-DMBD MOFs/3D-KSC could work efficiently in real water sample, and the treated Hg ion in water was lower than national discharge standard of industrial wastewater.

3.1.2. Cadmium treatment. Besides mercury, there are other metal cations that are harmful for aqueous environment and are necessary to be monitored and controlled.[94] Compared with traditional materials for adsorption, degradation and sensing severally, MOFs can offer a platform to integrate each function in one system and realize multi treatment towards metal ions. Cadmium is deemed to have bad effect to skeletal and nervous systems, and can lead to cancers.[95] In a research work by Hong and co-workers, A novel MOFs, FJI-H9 was fabricated by the combination of CaCl$_2$ and 2,5-thiophenedicarboxylate (Fig. 3).[96] FJI-H9 demonstrated a large adsorption capacity of 225 mg g^{-1}, together with good selectivity when coexisted with Ca^{2+}, Mg^{2+}, Co^{2+}, Ni^{2+}, Mn^{2+}, Zn^{2+}, Fe^{2+} and Pb^{2+}, and only two examples of MOFs for Cd^{2+} removal were reported before with moderate adsorption capacity.[97,98] Besides the removal ability, FJI-H9 also showed effective fluorescence quenching ability of Cd^{2+} and low concentrations down to 10 ppm could be detected within 10 min, and also displayed excellent selectivity toward other competing metal ions such as Hg^{2+}, Mg^{2+}, Co^{2+}, Ni^{2+}, Mn^{2+}, Zn^{2+}, Fe^{2+} and Pb^{2+}. Further investigations revealed that an unusual synergy stems from the electronegative framework and the suitable sized square cavity of FJI-H9 played an important role for the interaction with Cd^{2+}. And the reusability gave FJI-H9 potential for practical application in removal and sensing of Cd^{2+} in water.

Composite materials can integrate each function of their component and acquire multi functions, thus leading to synergistic effects.[99] He's group developed a Fe$_3$O$_4$/MOF/cysteine composite by synthesizing Cu-based MOFs outside nano Fe$_3$O$_4$, following by modifications of L-cysteine.[100] The Fe$_3$O$_4$ part in the material help realize fast separation from water with the help of a magnet. The maximum adsorption capacity was 248.2 mg g^{-1}, and the Fe$_3$O$_4$/MOF/cysteine can also be regarded as a fluorescent quenching sensor for detection of Cd^{2+} with the detection of limits of 0.94 ng mL^{-1}. In this composite, the high surface area and pore volume of MOFs offered a space to accommodate the target and L-cysteine, which had three functional groups (–SH, –NH$_2$, –COOH) that may offer binding site toward Cd^{2+}. Besides, L-cysteine help increase the fluorescent intensity of the MOF, which facilitate the Fe$_3$O$_4$/MOF/cysteine to be used as a turn off probe for Cd detection. The materials maintained above 90% efficiency after 5 times of reuse. Furthermore, a magnetic solid-phase extraction method was established using the MOF composites to detect trace Cd^{2+} ion in water. The limit of detection of 10.6 ng mL^{-1} was achieved. Fe$_3$O$_4$/MOF/cysteine was used to extract Cd^{2+} in tap water and lake water and showed potential for practical applications.

3.1.3. Lead and copper treatment. Pb^{2+} and Cu^{2+} are also common cation metal ion pollutions. In a research work by Wang's group, the amino-functionalized MIL-101 (Fe) was constructed through a one-step reaction of FeCl$_3$ 6H$_2$O and 2-aminoterephthalic acid.[101] The obtained MIL-101-NH$_2$ displayed good adsorption ability in removing Cu^{2+} and Pb^{2+} in water and the adsorption capacity reached 0.9 and 1.1 mM g^{-1}, respectively. Fluorescence quenching performance was also observed with a low limit of detection of 0.0016 and 0.0052 mM for Cu^{2+} and Pb^{2+}, respectively. The experimental results revealed that the chelation between amine groups in organic ligands and the target metal ions may induce interactions and host–guest electron transfer, causing the adsorption behavior and fluorescence quenching. The MIL-101-NH$_2$ maintained adsorption capacity with a slight decrease after six reuse cycles. Other MOFs synthesized from the same linker but different metal/metal clusters including MIL-101-NH$_2$(Cr), MIL-53-NH$_2$(Al), UiO-66-NH$_2$(Zr) and MOF-5-NH$_2$(Zn) demonstrated similar removal and sensing performance of Cu^{2+} and Pb^{2+}. The research showed such
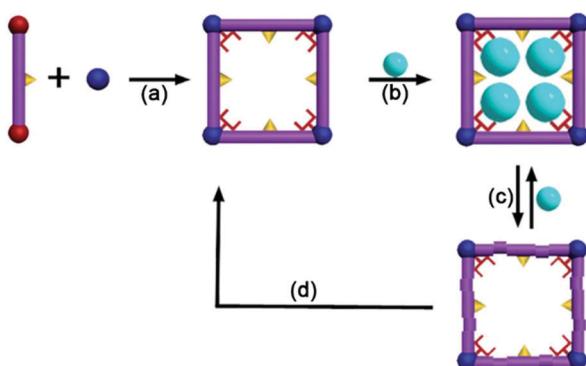
Fig. 3 A regenerative MOF for reversible uptake of Cd(II): (a) self assembly 3D framework from organic ligand and hard metal ion; (b) effective absorption with high capacity; (c) absorption and desorption; (d) reconstruction of the used sample into a fresh sample. Reproduced from ref. 96 with permission from Royal Society of Chemistry, copyright 2016.

serious of MOFs had potential for sensing and removal of Cu^{2+} and Pb^{2+} ions simultaneously in aqueous solution.

3.1.4. Radionuclide treatment. Spent nuclear fuel reprocessing, nuclear reactor operation, nuclear accidents, and nuclear weapon testing discharged bountiful radioactive nuclides, for example, ^{79}Se, ^{99}Tc, ^{90}Sr, ^{137}Cs, ^{235}U, ^{85}Kr, ^{127}Xe and $^{129/131}I$. These radioactive substances can cause gene mutation and destruction of biological system, and pose severe threats to both environment and public health.[102] Therefore, detection and removal of radionuclide is of great significance.[103] MOFs display excellent porosity, chemical stability and designability, and show great potential for radionuclide treatment.[3,104,105] The simultaneous detection and removal of radioactive substances can be achieved on MOFs *via* elegant design. To this end, Wang and co-workers synthesized a water-stable mesoporous terbium-based MOF to sense and remove uranyl ions in water.[106] To be specific, $Tb(NO_3)_3\cdot6H_2O$ and H_3TATAB (4,4′,4″-(1,3,5-triazine-2,4,6-triyltriimino)tris-benzoic acid) were used to construct Tb-MOF, whose channels were 27 Å × 23 Å and were equipped with abundant exposed Lewis basic sites (Fig. 4). Such Tb-MOF showed efficient quenching towards uranyl ions with good selectivity and the limit of detection reached 0.9 µg L^{-1}, far below the maximum contamination standard of 30 µg L^{-1} in drinking water defined by the United States Environmental Protection Agency. Tb-MOF also demonstrated efficient removal of uranyl ions with the adsorption capacity of 179.08 mg g^{-1}. Experiment results and DFT calculations revealed that the removal and sensing ability originated from the selective binding of uranyl ions onto the Lewis basic sites of the Tb-MOF. The great capability in uranyl ions detection in real water samples endows such Tb-MOF great potential in uranyl ions treatment.

Ratiometric detection hold advantage in sensing. The same group of Wang and co-workers reported a ratiometric monitoring of Thorium contamination in natural water using a dual luminescent Eu-MOF.[107] The obtained MOF ThP-1 showed highly sensitive and selective self-calibrated sensing of Th^{4+}, with the emission intensity increased at 617 nm and decreased at 365 nm. ThP-1 showed a wide detection range (0–300 mg L^{-1})


Fig. 4 Schematic for the formation of Tb-MOF for the adsorption and detection of uranium from aqueous solution. Reproduced from ref. 106 with permission from American Chemical Society, copyright 2017.

and low detection limit (24.2 µg L^{-1}), much lower than the thorium contamination standard of 246 µg L^{-1} in drinking water defined by the World Health Organization. ThP-1 also displayed selectivity of Th^{4+} towards Na^+, K^+, Cs^+, Mg^{2+}, Ba^{2+}, Sr^{2+} and Ca^{2+}. ThP-1 demonstrated Langmuir adsorption of Th^{4+} with the adsorption capacity of 25.82 mg g^{-1} and the adsorption also showed good selectivity towards the metal ions above. Experiment results combined with DFT calculations revealed that the selective uptake of Th^{4+} by the host ThP-1 through inner-sphere coordination were responsible for the sensing and removal process. Furthermore, ThP-1 could be used in real water samples, offering an option for simultaneous detection and removal of Th^{4+} in aqueous solution.

Single-crystal to single-crystal (SC–SC) transformation of MOFs has caused great interest, as it allows creation of new materials and postsynthetic functionalization of MOFs in a stepwise and visualizable manner.[108] Lin and co-workers synthesized a cationic thorium MOFs showing triple SC-SC transformation in organic solvents, water and $NaIO_3$ solution.[109] Thereinto, the SC–SC transformation in $NaIO_3$ solution can cause turn-off sensing of IO_3^- ion. The Th-MOF showed the detection limit of 0.107 µg kg^{-1} of iodate and demonstrated good anti-interference towards a serious of cation and anion ions (BO_3^{3-}, SO_4^{2-}, CO_3^{2-}, F^-, Cl^-, HCO_3^-, NO_3^-, Na^+, K^+, Ba^{2+}, Sr^{2+}, Ca^{2+}, Zn^{2+}, Mg^{2+} and Al^{3+}). Besides sensing, Th-MOF also displayed efficient removal of IO_3^- with the adsorption capacity of 152.6 mg g^{-1} and the fast adsorption equilibrium within 30 min. The sensing mechanism can be explained as the SC–SC transition induced by IO_3^- caused the large modifications of the ligand conformation and turned the ligand-based emission off. Besides, the host–guest interaction between the luminescent framework and IO_3^- leads to heavy atom induced intersystem crossing, resulting in a selective and static quenching by a distinct mechanism. The SC–SC transition on such Th-MOF offered an alternative way to simultaneous detect and remove IO_3^- in aqueous solution.

MOF-based composites materials can also assist in radionuclide treatment. Wang's group designed a composite material made of a magnetic core and a zeolite imidazolate framework (ZIF-8) shell surrounded by carbon dots (CDs) to simultaneous sensing and removal of uranium ion in water.[110] Fe_3O_4-CMC@ZIF-8@CDs had a large adsorption capacity of 606.06 mg g^{-1}. Moreover, the fluorescence intensity decreased close to detection limit as the U(VI) concentration increased to 100 mg L^{-1}. Experimental data showed that ZIF-8@CDs part offered large surface area and abundant nitrogen/oxygen sites on the surface, and the main interaction mechanisms are diffusion and coordination. Na_2CO_3 containing H_2O_2 solution can serve as desorption agents, and the Fe_3O_4-CMC@ZIF-8@CDs can be reused for at least 5 cycles with high adsorption efficiency, giving such material great potential in uranyl ion multiple treatment.

3.1.5. Oxyanions treatment. Cr^{6+} oxyanions, *viz.*, dichromate ions are most common oxyanions pollutions in water environment. Cr(VI) compounds are classified as "Group A" of human carcinogens by World Health Organization (WHO), which are proved to have carcinogenic effect to human. Therefore, detection and control the content of Cr^{6+} oxyanions in water is
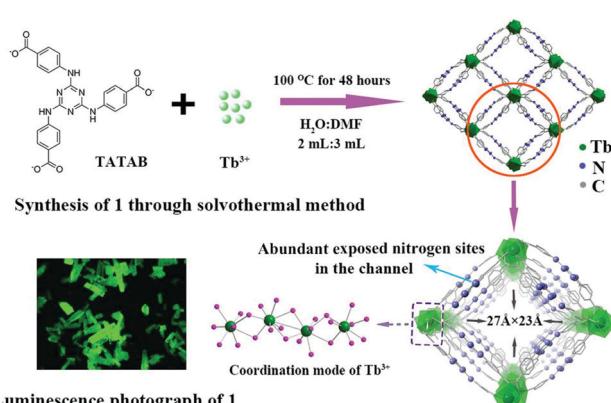
extremely necessary and important.[111,112] Zr-based MOFs are famous for their water stability and accessibility on a wide pH range, and are frequently used in Cr^{6+} oxanions pollution treatment. Li's group developed a stable luminescent MOFs for simultaneous removal and detection of dichromate ions in water. In this work, a new Zr-based MOFs, BUT-39 was synthesized *via* the reaction of a T-shaped organic ligand, H_3BTBA, with zirconium salt and a rarely (3,9)-connected Zr-MOF was obtained.[113] BUT-39 showed good water stability in boiling water, pH 12 NaOH solution and 2M HCl solution. BUT-39 displayed excellent fluorescence quenching performance to $Cr_2O_7^{2-}$, with a low detection limit of 1.5 μM and a short response time of less than 1 min. This MOF demonstrated high selectivity towards $Cr_2O_7^{2-}$ compared with other anions like F^-, Cl^-, Br^-, I^-, NO_2^-, NO_3^-, ClO_4^-, IO_3^-, AcO^-, CO_3^{2-}, SO_4^{2-}, MoO_4^{2-}, WO_4^{2-} and PO_4^{3-}. The luminescence quenching might be a synergetic effect from both the competitive absorption on excitation light and the energy transfer between BUT-39 and $Cr_2O_7^{2-}$. Meanwhile, BUT-39 also showed good removal ability to capture $Cr_2O_7^{2-}$ rapidly within 1 min, together with a high adsorption capacity of 215 mg g^{-1}. Besides, BUT-39 showed a good anti-interference ability in $Cr_2O_7^{2-}$ adsorption with the other anions appeared above. The coordination between Zr_6 cluster and $Cr_2O_7^{2-}$, and the basic imidazole N atoms in benzimidazole moieties can form a protonated salt in acid solution, being favorable to enrich negative $Cr_2O_7^{2-}$. BUT-39 can be an ideal candidate for fast and selectively removal and sensing $Cr_2O_7^{2-}$ in water.

Ratiometric detection induced by dual emissions can eliminate interferences from the surrounding environment and is widely used in ions sensing.[114] In another research of Zr-based MOFs synthesized by Choi and co-workers, two types of dyes, 7-amino-4-methylcoumarin and resorufin with two different emissions were introduced into a MOF consist of fumarate and Zr cluster, *viz.*, MOF-801 (Fig. 5).[115] The dyes offered a dual fluorescence emission for the ratiometric detection and the porous MOF-801 was conducive to effect removal of the target. The obtained Dyes⊂MOF-801 material showed a $Cr_2O_7^{2-}$ adsorption capacity of 83 mg g^{-1} and the process can be finished within 3 min, even in the presence of excess metal ions and anions (Cl^-, NO_3^-, CO_3^{2-}, SO_4^{2-}, PO_4^{3-}, and citrate) with 10-fold excess concentrations. Besides, fluorescence intensity ratio of coumarin over resorufin in Dyes⊂MOF-801 was used as ratiometric detection for $Cr_2O_7^{2-}$, as the two dye molecules within MOF-801 can both detect $Cr_2O_7^{2-}$ at different emissions. A detection limit of 0.03 mM was achieved and a high selectivity was attained even in the presence of a 260-fold excess of interfering ions on Dyes⊂MOF-801, exhibiting strong anti-interference capability.

Membranes play an important role in wastewater separation. MOFs based membranes can combine the high surface area, porosity and functionality of MOF and the easy maintenance, strong adaptability, small footprint and high separation efficiency of membrane, offering attractive prospect in water pollution treatment.[116] Cui's group developed MOF-based mixed-matrix membranes (MMMs) for simultaneously removal and sensing of $Cr_2O_7^{2-}$ in aqueous system.[117] To be specific, a water stable cationic Eu-based MOF (Eu-mtb) was mixed with poly (vinylidene fluoride) to form MOF-based MMM. The obtained Eu-mtb MMM showed efficient removal ability towards $Cr_2O_7^{2-}$ with the adsorption capacity of 33.34 mg g^{-1}. In addition, fluorescence sensing behavior of Eu-mtb MMM to $Cr_2O_7^{2-}$ was also achieved, with the detection limit of 5.73 nM. The MMMs helped Eu-mtb to distribute uniformly without aggregation and make it possible for the sufficient interactions between $Cr_2O_7^{2-}$ and Eu-mtb MOF. As a result, the adsorption capacity and sensing sensitivity were both enhanced compared with bare Eu-mtb. The competitive adsorption and resonance energy transfer may response for the sensing behavior. Eu-mtb MMM also manifested good selectivity when anions like Cl^-, NO_3^- and I^- caused small interference in both adsorption and sensing towards $Cr_2O_7^{2-}$.

As non-degradable properties of metal ions, catalytic redox reactions that transform the metal valence to a low-toxic state offers an effective way for inorganic pollution treatment. For example, dichromate ions are highly toxic, but their reduction products, Cr^{3+} ions are much less toxic.[118] Functional MOFs can serve as a catalytic media for the reduction of Cr^{6+} oxanions.[119] Gu and co-workers constructed a serious of UiO-66 type MOFs with different hydroxyl groups (UiO-66-OH, UiO66-$(OH)_2$).[120] The hydroxyl groups on organic ligands played a vital role in Cr(VI) treatment, as UiO66-$(OH)_2$ showed an adsorption capacity of 53.8 mg g^{-1}, larger than that in UiO-66-OH of 16.1 mg g^{-1}. Meanwhile, a reduction process can occur *in situ* on the Cr(VI) adsorbed MOFs and Cr(III) was detected as a less toxic product. The abundant hydroxyl groups can serve as not only reductive sites for the conversion of Cr(VI) to Cr(III), but also intrinsic anchors for the enhanced adsorption of Cr(VI). When simulated industrial wastewater containing 5 mg L^{-1} Cr(VI) was treated with UiO66-$(OH)_2$, less than 50 μg L^{-1} Cr(VI) could be detected, making this material promising candidate for removal and reduction of Cr(VI) in
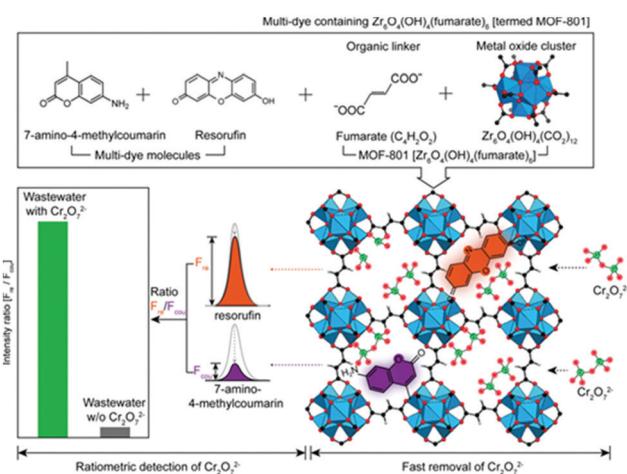
Fig. 5 Schematic of the ratiometric detection and simultaneous removal of $Cr_2O_7^{2-}$ using multi-dye (resorufin and 7-amino-4-methylcoumarin) containing MOF-801. Reproduced from ref. 115 with permission from Elsevier Inc, copyright 2019.

water. Afterwards, the same group developed a universal strategy of introducing thiol groups into MOFs for Cr(VI) removal and reduction in water.[121] For details, thiol-containing Zr-MOFs was fabricated using mercaptosuccinic acid (MSA) and *meso*-dimercaptosuccinic acid (DMSA) as organic ligands. The thiol groups played an important role in simultaneous removal and reduction of Cr(VI), as Cr(VI)–thiolate complex formed to facilitate the adsorption process and the oxidation of thiol groups helped to reduce Cr(VI) to Cr(III), respectively. As a result, adsorption capacity of 202.0 and 138.7 mg g^{-1} was acquired for Zr-MSA and Zr-DMSA, respectively. By virtue of UV-Vis spectra and XPS measurement, Cr(III) was detected after the Cr(VI) was adsorbed on the MOF, indicating a reduction of Cr(VI) on MOFs. The thiol-containing MOFs showed good anti-interference when other ions coexisted. Moreover, such thiol-introducing strategy is universal for other MOFs such as UiO-66 and MOF-808, which provided a guideline for design Cr(VI) multiple treatment MOFs in aqueous environment. However, the catalytic reduction of Cr(VI) was not discussed in detail on the above two works.

Materials that can realize sensing, removal and degradation functions simultaneously are highly desirable, as the overall treatment from "birth" to "death" of water pollutions can be achieved on one material. However, such process made high requests for material design and preparation. To this end, Liu and co-workers made an effort to employ a multifunctional Zr-based MOFs for efficient detection and removal of Cr(VI) in water solution. In this work, a highly water stable luminescent MOF consists of 2,3,5,6-tetrakis(4-carboxyphenyl)pyrazine (H$_4$TCPP) and Zr clusters, namely, JLU-MOF60 was successfully constructed (Fig. 6).[122] The sqc topology Zr-MOF showed extensive pH stability from 0 to 11 and is ideal for applications in water. As Zr-bonded hydroxides have high affinity to $Cr_2O_7^{2-}$, JLU-MOF60 displayed a high adsorption capacity of 149 mg g^{-1} as well as fast adsorption rate of 38 mg g^{-1} min^{-1} towards $Cr_2O_7^{2-}$, and showed excellent anti-interfering without losing much of its adsorption capacity when competing anions such

as Cl^-, Br^-, I^-, NO_3^-, SO_4^{2-} and PO_4^{3-} coexisted in aqueous solution. Furthermore, with the help of the aggregation induced emission (AIE) effect of the organic H$_4$TCPP ligands, JLU-MOF60 can not only sense $Cr_2O_7^{2-}$ through luminescence quenching, but also photodegrade Cr(VI) to Cr(III) in water. For sensing, the detection limit can reach as low as 9.38 μM with good anti-interference ability of other anions, *e.g.*, F^-, Cl^-, Br^-, I^-, PO_4^{3-}, NO_2^-, NO_3^-, MoO_4^{2-} and VO_3^-. For photocatalytic reduction, 98% Cr(VI) converted to Cr(III) after 70 min of light exposure, and the rate constant κ was determined to be 0.058 min^{-1}, showing an effective photocatalytic property. This work offered an efficient method for design and synthesize multi-functional MOFs for simultaneously sensing, removal and degradation of Cr(VI) in water.

3.1.6. Halide ions treatment. Halide ions such as fluoride ion and iodide ion are turned out to be hazardous to both environment and human health. Excess or shortage of iodine is both harmful for thyroid, and overexposure to fluoride can bring about acute gastric and kidney problems.[123] Excessive fluoride ions have been in connection with debilitating bone disease fluorosis.[124] Therefore, monitoring the content and conducting effective removal measures is of great importance in water. Zhang's group used a typical MOFs, NH$_2$-MIL-53(Al) to simultaneous sensing and removal of fluoride anions.[125] NH$_2$-MIL-53(Al) showed a high adsorption capacity of 202.5 mg g^{-1}, and the adsorption equilibrium was finished within 60 min. Moreover, NH$_2$-MIL-53(Al) displayed fluorescence enhancement towards F^- with the detection limit of 0.31 μmol L^{-1} and a wide detection range of 0.5–100 μmol L^{-1}. The specific bonding between fluoride and Al metal may result in the adsorption process and the bonding may interrupt the electron transfer between organic ligands and Al, causing fluorescent enhancement. Such MOFs was used to detect in practical water samples and acquired satisfying recoveries of 89.6–116.1%, holding prospects in F^- treatment in wastewater.

In a recent work, Li and co-workers explored a novel In-based MOF, In(tcpp) using a chromophore ligand, 2,3,5,6-
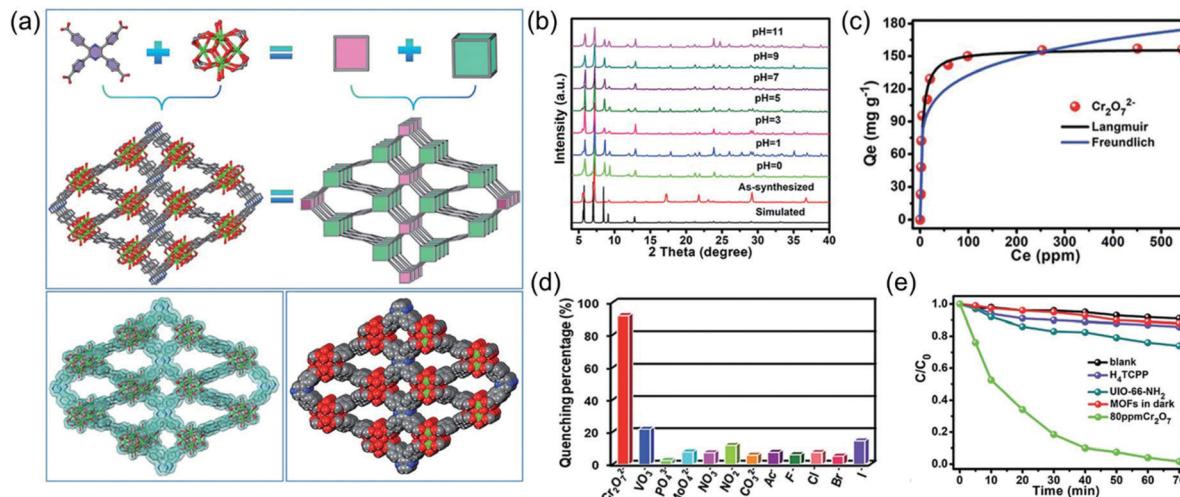
Fig. 6 (a) The structure illustration of JLU-MOF60; (b) the stability of JLU-MOF60 in various pHs; (c) the removal ability; (d) the sensing ability and (e) the degradation ability of JLU-MOF60 for $Cr_2O_7^{2-}$ treatment. Reproduced from ref. 122 with permission from Royal Society of Chemistry, copyright 2019.
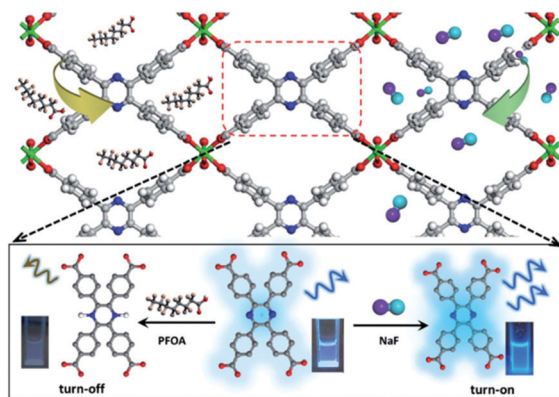
Fig. 7 The structure of In(tcpp) and schematic presentation of its luminescence switchable turn-off response toward PFOA and turn-on response toward F ions. Reproduced from ref. 126 with permission from Royal Society of Chemistry, copyright 2021.

tetrakis(4-carboxyphenyl)pyrazine (H$_4$tcpp) (Fig. 7).[126] The In(tcpp) showed dual functions for sensing and removal of fluorinated chemicals. Specifically, In(tcpp) displayed a turn-on detection of F$^-$ within 5 min and showed a limit of detection of 1.3 μg L^{-1}. In(tcpp) also exhibited excellent anti-interference against various cations and anions such as Ag$^+$, Cd^{2+}, Co^{2+}, Cu^{2+}, Ni^{2+}, Pb^{2+} Fe^{3+}, Al^{3+}, Cl$^-$, Br$^-$, NO$_2^-$, NO$_3^-$, SO$_4^{2-}$, PO$_4^{3-}$, CN$^-$ and acetate. Besides, In(tcpp) can serve as an adsorbent for the removal of F$^-$ with a adsorption capacity of 36.7 mg g^{-1}. Experiments and DFT calculations revealed that the interaction between F$^-$ and In(tcpp) mainly occurred at the bridging –OH$^-$ offered by organic ligands. The reusability makes In(tcpp) promising materials for fluorinated chemicals treatment in aqueous solution.

MOFs and MOF-based composites have shown potentials for multiple treatment for inorganic pollutions, as more than one function of sensitive sensing, efficient removal and detoxication can be realized. However, some improvements can still be made, for example, exploiting sensitive turn on sensing modes and improving the reusability performance towards metal ions.

3.2. MOFs for multiple treatments of organic pollutions in water

Compared with inorganic pollutions, the organic pollutions are more abundant and diverse in water environment, including dyes, pharmaceuticals and personal care products (PPCP), pesticides, persistent organic pollutants (POPs), endocrine-disrupting compounds (EDCs) and emerging organic contaminants (EOCs).[127] These organic pollutions can cause adverse effect to water environment and organisms and bring mutagenesis, carcinogenesis and teratogenesis to human.[128] Therefore, detection and removal of organic water pollution is significant. MOFs have the advantages of porosity, designability, easy functionalization and tunability, which are ideal materials suited for introducing multiple functions on organic water pollution treatment.[129]

3.2.1. Dyes treatment. Dyes are in large demand in textiles, plastics, paper, cosmetics and other industries, and many of which have discharged to water, causing toxic and carcinogenic

properties to environment and human health. In addition, their intense color reduces sunlight to enter into water, thus interfering the ecosystem.[130,131] It is important to detect, remove and finally degrade the organic dyes in water environment. As organic dyes are the most studied organic pollution in water, researchers have made many efforts to explore functional materials for dyes sensing, removal and degradation. Fe has the catalytic property and the Fenton reaction it participated is widely used in organic pollution degradation.[132] Integration of Fe into MOFs is a workable way to introduce catalytic behaviors.[133] To this end, Guo's group synthesized a serious of Fe-based MOFs, namely MIL-101(Fe), MIL-100(Fe), MIL-53(Fe) and MIL-88B(Fe), to serve as both adsorbents and catalysts for acid orange 7 (AO7) treatment.[134] The four MOFs all showed efficient adsorption ability toward AO7, with the adsorption capacity from 153.4 to 31.4 mg g^{-1} in the order of MIL-101(Fe) > MIL-100(Fe) > MIL-53(Fe) > MIL-88B(Fe). This is in accordance with the surface area order of the four MOFs from 2986 to 19.2 m^2 g^{-1}, and the results demonstrated the importance in porosity during the adsorption of AO7 in the four MOFs. For the degradation, persulfate was introduced to assist the process, and the Fe site could efficiently activate persulfate to produce •OH or SO$_4^-$•. Larger surface area helped more targets to contact with Fe sites in MOFs and favors the catalytic process. As a result, the catalytic efficiency followed the same order of the adsorption order, with the rate constants κ from 0.017 to 0.003 min^{-1} Finally, the Fe-based MIL MOFs can be reused for at least three times without losing their catalytic or adsorption abilities, exhibiting promising potentials in AO7 control in water.

In another work by Li's group, Fe-loaded MOF-545(Fe) was explored as peroxidase-like activity for removal and degradation of dyes in water.[135] The experimental conditions were investigated in detail, and the degradation can be completed within 2 hours under optimized conditions in the presence of H$_2$O$_2$. Fe-loaded MOF-545(Fe) also displayed good removal ability, with the adsorption capacities of methylene blue and methyl orange reaching 382.35 and 803.66 mg g^{-1}, respectively. The Fe-loaded MOF-545(Fe) demonstrated good reusability, which is crucial for practical application.

Yu's group constructed iron–nickel bimetallic MOFs for removal and photo-Fenton degradation of dyes in aqueous
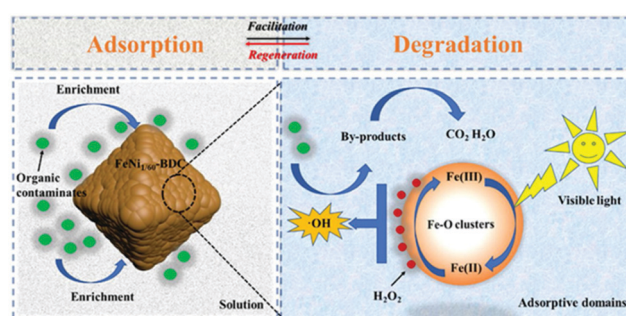

Fig. 8 Schematic illustration of contaminant removal in FeNi$_{1/60}$-BDC/H$_2$O$_2$/visible light system. Reproduced from ref. 136 with permission from Elsevier Inc, copyright 2021.

solution (Fig. 8).[136] With the Ni doping in MIL-101(Fe), the obtained FeNi$_{1/15}$-BDC showed 5.2 and 2.6 times larger in adsorption capacity for MB and MO, respectively, due to the enlarged pore volume and specific surface area. Slow induction stage and rapid oxidation stage on the degradation process of FeNi$_{1/15}$-BDC was found to fit with pseudo-zero-order kinetics. And the increased degradation rate constants were observed by FeNi$_{1/15}$-BDC (2.472 *vs.* 1.188 min^{-1} for MB; 0.616 *vs.* 0.421 min^{-1} for MO). Notably, the FeNi$_{1/15}$-BDC displayed wide working pH range and reusability, and can be used for the reinforced removal and degradation of organic dyes.

MOF composite materials also contribute to the multiple treatment of dyes. Basu's group fabricated a silica supported bimetallic MOF, *viz.*, MIL-53(Al-Fe)@SiO$_2$ to realize adsorption and photocatalytic degradation of methylene blue (MB).[137] SiO$_2$ assisted in increasing the photocatalytic activity and the composites outperformed the pure MIL 53 (Al). As Fe, Al and SiO$_2$ coexisted in MIL-53, the electron and hole recombination was inhibited and the band gap was reduced. As a result, 99.85% of MB was photodegraded with satisfactory recyclability. Besides, a large maximum adsorption capacity of 681.78 mg g^{-1} was acquired, also with good reusability.

Another example of MOF-based hybrids for dye treatment was reported by Meng and co-workers. Gold nanorods/MOFs (AuNRs/Fe-MOF) composite was successfully developed for sensing and degradation of MB (Fig. 9).[138] The catalytic activity of Au NRs/Fe-MOF was notably improved compared with pure MOFs. AuNRs in the composites could facilitate electrons transferred from Au to MOF, resulting reduction of Fe(III) to Fe(II) on MOFs and Fenton reaction by Fe^{3+}/Fe^{2+} was activated. Thereby, an excellent rate constant (k = 0.182 min^{-1}) and good degradation rate (5 μM MB, completely degraded within 20 min) was observed with the presence of H$_2$O$_2$. Interestingly, Au NRs/Fe-MOF can display chemical and electromagnetic

enhancement of Raman signals towards MB. Fe-MOF can accept electrons from Au NRs under localized surface plasmon resonance (LSPR) excitation and the electron–hole recombination is prohibited. Therefore, Raman signal is enhanced through a charge-transfer mechanism with the help of Au NRs. The detection limit of MB is 9.3 × 10^{-12} M, showing ultra-low sensitivity, thus causing enhancement on both catalytic and Raman signals. Considering the excellent stability and reusability, Au NRs/Fe-MOF can serve as a promising material for dye detection and degradation in water.

Membrane materials can facilitate dye treatment as well. Balakrishna's group developed photocatalytic MOF-integrated polysulfone (PSF) membranes for separation and degradation of organic dyes in water (Fig. 10).[139] NH$_2$-MIL-101(Fe) was synthesized to enhance the optical properties and control the surface charge. This Fe-MOF was then embedded into PSF membrane, and the obtained MOF-integrated membrane was used for separation, removal and degradation of RhB and MO. The membrane could make NH$_2$-MIL-101(Fe) devices and improved water flux and good rejection was achieved. Antifouling capacity was largely increased and above-par, reaching flux recovery ratio values above 95%. Compared with the bare membrane with 20–30% rejection and 0% degradation efficiency of dyes, the MOF-integrated membrane displayed around 80–100% rejection as well as 10 and 18% degradation efficiency to MO and RhB, respectively. The good water flux and antifouling capacity made such MOF membrane promising candidates for wastewater treatment.

Apart from Fe-based MOFs, other MOFs can also serve as multifunction platform for anionic dye treatment. Zheng and co-workers developed SCNU-Z2 based on a heterotopic tripodal nitrogen-containing ligand and Co(II).[140] The imidazole group was replaced by the tetrazole group and the framework charge
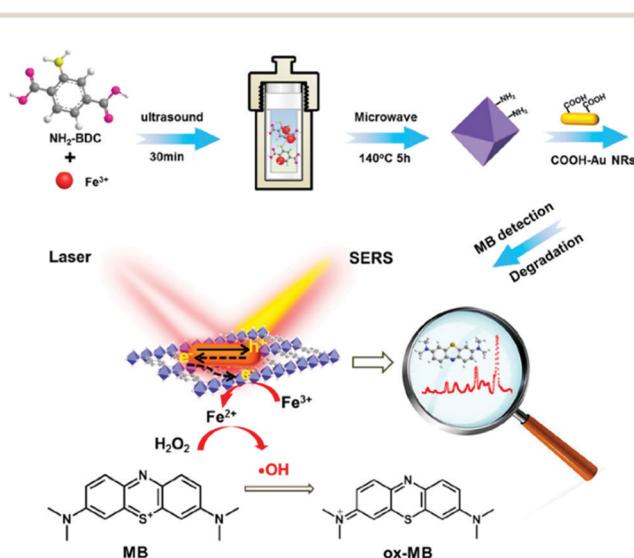
Fig. 9 Schematic diagram of the preparation of Au NRs/Fe-MOFs for methylene blue *in situ* catalytic degradation and SERS detection. Reproduced from ref. 138 with permission from American Chemical Society, copyright 2022.
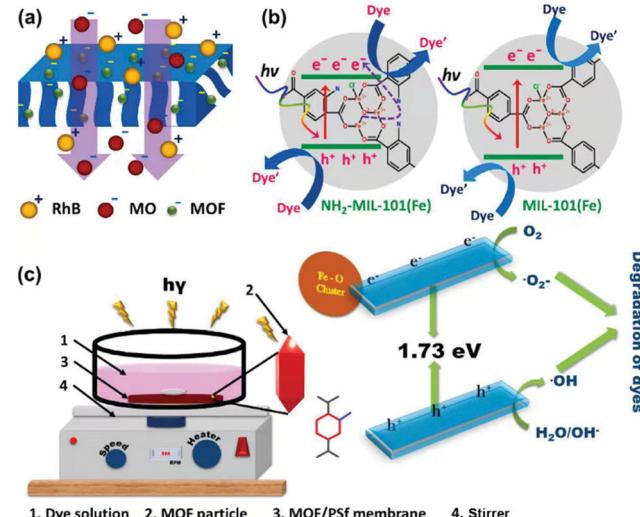

Fig. 10 Schematic illustration of (a) rejection and (b) photocatalytic degradation of dye molecules over the NH$_2$-MIL-101(Fe) and MIL-101(Fe) MOF-integrated membranes and (c) pictorial illustration of degradation setup and its mechanism. Reproduced from ref. 139 with permission from Elsevier Inc, copyright 2022.

is turned to anionic. The SCNU-Z2 showed high stability in wide pH range from 3 to 11, and the anionic character enables the efficient removal for cationic dyes, *viz.*, Methylene Blue (MLB), Crystal Violet (CV) and Rhodamine B (RhB) with the large adsorption capacity of 455.6, 847.4 and 751.8 mg g^{-1}, respectively. In contrast, SCNU-Z2 displayed extremely low adsorption to anionic dyes and can be used for cationic and anionic dyes separation. Interestingly, SCNU-Z2 demonstrated degradation behavior towards MB, and the degradation rate can reach 97% in the darkness within 15 min. However, A deep understanding of the degradation mechanism needs to be further explored.

Ce-based MOFs that suited for the treatment of both cationic and anionic dyes are explored by Cai's group. In this study, Ce-UiO-66 was explored as adsorbent to remove and degrade MB, MO, RhB and AO7.[141] Ce-UiO-66 had an adsorption capacity of 243, 288, 583 and 413 mg g^{-1} to MB, MO, RhB and AO7, respectively, which is increased by 3–4 times compared with Zr-UiO-66. Experiment results and DFT calculations revealed that π–π interactions existed between the four dyes and Ce-UiO-66. Electrostatic interaction played vital role for the adsorption of cationic MB and MO in Ce-UiO-66. For anionic RhB and AO7, hydrogen bonding and Ce–O were the main mechanisms. Subsequently, the removal rate of MB, MO, RhB, and AO7 by Ce-UiO-66 was significantly improved, and the degradation rates were 81%, 89%, 99% and 98%, respectively, within 60 min under UV irradiation. Investigation of the degradation mechanism showed that the negative ligand-to-metal charge transfer (LMCT) accelerated the separation of electron–hole pairs and caused effective degradation of organic dyes. The reusability and water stability combined with removal and degradation ability endowed such MOFs potential practical applications in wastewater treatment.

The exploration of Indium-based MOF for removal and degradation of dyes was conducted by Zhai and co-workers. SNNU-110 was synthesized using an amino-functional linker and In clusters.[142] Under irradiation, SNNU-110 exhibited good photocatalytic behavior toward RhB and MB, with the degradation efficiency of 94.6% for RhB and 93.1% for MB. The inorganic [In$_3$O] cluster endowed SNNU-110 with good photocatalytic activity. The framework formation played a critical role in the degradation process, as in a control experiment, pure In$_2$O$_3$ displayed little photocatalytic activity to RhB and MB. Interestingly, SNNU-110 also showed fluorescence quenching performance for six nitroaromatics with good repeatability. SNNU-110 can be used as a multifunctional material for dyes elimination and nitroaromatics sensing.

Rare earth-based MOFs can also assist in dye elimination. Zhang and co-workers fabricated two rare earth MOFs from the reaction of Eu^{3+} and Tb^{3+} with an aromatic tetracarboxylic acid (TPTC).[143] The two MOFs displayed pH stability in the range of 3–9 and the negative zeta potential enabled the Eu-TPTC and Tb-TPTC to selective adsorption and degradation of cationic and neutral dyes. Eu-TPTC showed removal efficiency of 96%, 92%, 93% and 85% for cationic MB, CV, RhB and neutral dye, neutral red (NR), respectively. The two MOFs also showed good

photocatalytic degradation towards the dyes mentioned above, with all the degradation efficiency greater than 94%. The mechanism indicated that $^{\bullet}$OH and $^{\bullet}$O$_2$$^-$ increased the sensitization of dyes and the separation of photogenerated carriers, and promoted the efficiency of photocatalytic degradation.

3.2.2. Pesticide treatment. Pesticides are extensively used in agriculture and play a pivotal role in food protection and insect eradication. However, the residuals in water can cause adverse effect to environment as well as animals and plants.[144] As pesticides proved to reduce the activity of acetylcholinesterase and cause lesion to organs, they pose a great threat to public health. Thereby, developing effective methods to remove, detect and degrade toxic pesticides is highly anticipated.[145,146] To this end, MOFs can be exploited as a multi-function platform to monitor and eliminate pesticides. In an advanced work by Wang's group, a MOF-based composite was developed for simultaneous sensing and removal of glyphosate, an organophosphorus pesticide (Fig. 11).[147] Fe$_3$O$_4$@SiO$_2$@UiO-67 was constructed through a layer-by-layer assembly strategy. The Zr–OH groups in UiO-67 offered high affinity to phosphate groups in glyphosate, thus leading to high adsorption capacity and selective detection. As a result, Fe$_3$O$_4$@SiO$_2$@UiO-67 demonstrated a high adsorption capacity of 256.54 mg g^{-1} together with good reusability. The interaction between glyphosate and MOF caused fluorescence quenching in intensity, and the silica shell prevented electron transfer between UiO-67 and the magnetic core, hence resulting in the identification of the adsorbate and its concentration. Therefore, a lower limit of detection was acquired (0.093 mg L^{-1}). Furthermore, the magnetic core endowed the materials with convenience in fast separation with the help of the magnet and the composite material showed excellent water stability and repeatability in both sensing and removal process. The Fe$_3$O$_4$@SiO$_2$@UiO-67 integrated the advantages of the individual components and can be used as a promising material for simultaneous sensing and removal of glyphosate in wastewater.

Enzymes hold great potential in wastewater treatment, as they exhibit excellent selectivity, mild operating condition and
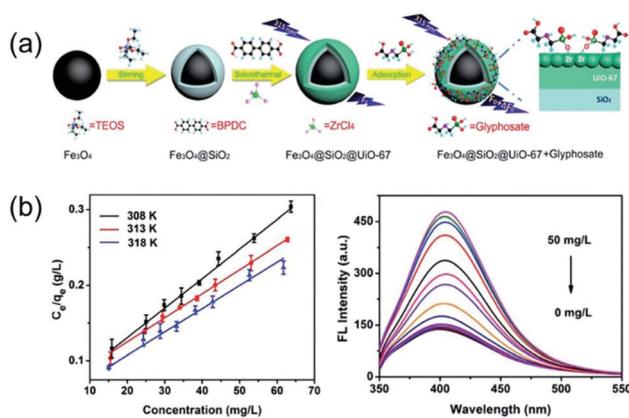

Fig. 11 (a) A schematic illustration of the fabrication of the Fe$_3$O$_4$@SiO$_2$@UiO-67 MOF-based adsorbent. (b) The adsorption and the detection performance for glyphosate treatment. Reproduced from ref. 147 with permission from Royal Society of Chemistry, copyright 2018.

high degradation efficiency.[148] However, as enzymes are sensitive to external environment, inactivation easily occurs to enzymes, and careful measures should be taken to protect the enzymes.[149] Due to their porosity, high surface area and functionality, MOFs can offer a good platform to encapsulate enzymes and improve their resistance to environment and the MOF–enzymes can hold promising applications in various fields.[150,151] For this purpose, Deep and co-workers constructed Terbium-BTC MOF to encapsulate hexahistidine-tagged organophosphate hydrolase (OPH[6His]) enzyme.[152] The MOF–enzyme was used to simultaneously detect and degrade an organophosphate pesticide, methyl parathion in water. The porous MOF played a part in protecting the enzyme and improving the adsorption ability towards the analyte. The OPH[6His]@Tb-BTC showed a 30% enhanced enzymatic activity compared with pure OPH[6His] and the good reusability for at least five cycles. An increased signal in UV-vis adsorption spectra was observed when methyl parathion was incubated with OPH[6His]@Tb-BTC, which is ascribe to the signal of the catalytic conversion products. A wide detection range of 0.1–1000 μM as well as a low detection limit of 2.6 nM was obtained. Moreover, a less toxic metabolite was formed via the catalytic conversion of methyl parathion, indicating a promising role of OPH[6His]@Tb-BTC in the detection and elimination of pesticide in aqueous environment.

3.2.3. PPCP treatment. As more and more commercial pharmaceutical and personal care products are exploited and used on human, PPCPs have become emerging pollutions in the recent decades. Excess PPCPs discharge into the water environment through groundwater, surface water, sewage and tap water and bring threat to humans and other living organisms, some of which proved to have adverse effect to humans.[153,154] Therefore, monitor and eliminate PPCPs in water holds great significance.[155] MOFs are suitable candidates for PPCP multiple treatment by virtue of their porosity, high surface area, tunable structures and easy functionalization.[156] Among PPCPs, Antibiotics are a broad spectrum antibacterial medicine that is widely used in animal and human infections treatment. However, the overuse of Antibiotics makes it excess in water environment and may cause hepatotoxicity, anaphylactic reaction, and gastrointestinal function disorder to people and antibiotic resistance in bacteria.[157] To be monitor and eliminate tetracycline (TC), a kind of antibiotics, Wang's group developed an Eu-based MOF containing characteristic metal chains through one step to simultaneous sensing and removal of TC (Fig. 12).[158] Interestingly, the Eu-MOF showed significant fluorescence enhancement with a wide range (0.05-60 μM) and low detection limit (3 nM) towards TC under optimized conditions. Meanwhile, the Eu-MOF also demonstrated good adsorption capacity of 387 mg g^{-1} for TC. Possible mechanisms containing host–guest interactions of Eu nodes, π–π interactions, electrostatic attraction and hydrogen bonding were further explored. Moreover, the recoveries of 94.89–112.86% was obtained in real water samples, indicating practical feasibilities in aqueous solution.

Another work to eliminate TC was reported by Yang and co-workers.[159] Depending on the catalytic behavior of Fe, three Fe-based MOFs, namely, Fe-MIL-101, Fe-MIL-100 and Fe-MIL-53 were synthesized to explored the degradation abilities of TC
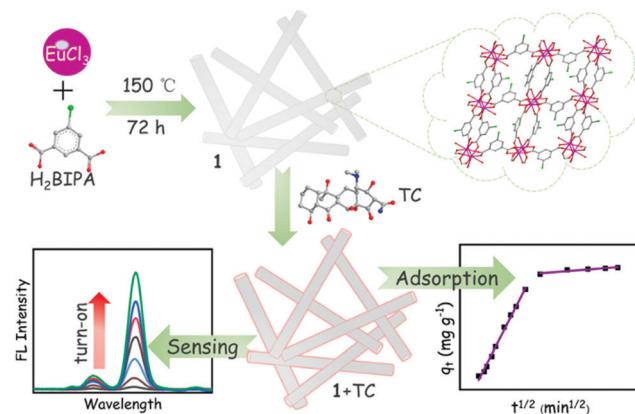

Fig. 12 Schematic procedure for the preparation of Eu-MOF for simultaneously sensing and removal of tetracycline. Reproduced from ref. 158 with permission from Elsevier Inc, copyright 2021.

on Fe-based MOFs. The experiment results showed that Fe-MIL-101 had the best removal efficiency of 96.6% compared to that of 57.4% in Fe-MIL-100 and 40.6% in Fe-MIL-53, respectively. Moreover, through the investigation of degradation conditions, Fe-MIL-101 showed excellent photocatalytic degradation performance when TC concentration was 50 mg L^{-1}. $^{\bullet}O_2^{-}$, $^{\bullet}OH$ and h^{+} were the main active species in photocatalytic degradation process of TC. The materials can be reused three times without losing its removal and degradation abilities.

MOF composites can also assist in TC treatment. Dai's group fabricated a p-type semiconductor-MOFs composite (CBO@ZIF-8) to sense and degrade TC in aqueous solution (Fig. 13).[160] Core-shell structure was obtained with a CuBi$_2$O$_4$ core and ZIF-8 shell. CBO@ZIF-8 showed an excellent fluorescence turn on effect towards TC at 517 nm emission, and a good linear range from 0 μM to 45 mM was obtained. The detection limit was as low as 26 nM and a fast response within 120 s, which can be applied for real-time monitoring of TC. The interfering experiment showed that antibiotics such as penicillin, cefradine, and levofloxacin caused little fluorescence
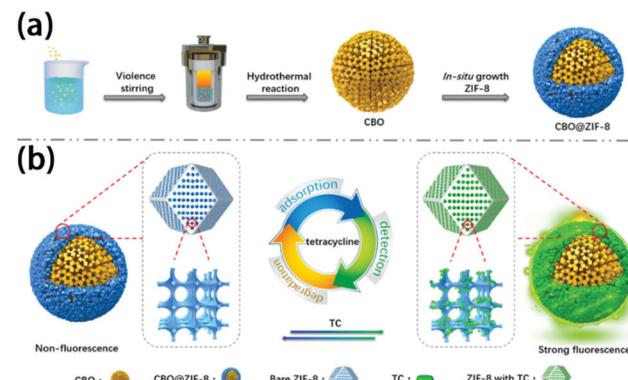
Fig. 13 Schematic illustration of (a) synthesis procedure of the CBO@ZIF-8 and (b) corresponding strategies of TC adsorption, detection, and degradation over CBO@ZIF-8. Reproduced from ref. 160 with permission from American Chemical Society, copyright 2020.

change on CBO@ZIF-8, indicating good selectivity of the material. The good sensing performance can be ascribed to the formation of a Zn-TC coordination compound between TC and ZIF-8. The photodegradation behavior of CBO@ZIF-8 displayed that 75.2% TC was decomposed after 120 min. The mechanism revealed that photogenerated electrons generated on CBO@ZIF-8 can be separated effectively to produce reactive oxygen species (ROS), which can further oxidize TC. In general, the ZIF-8 shell could generate sensing performance towards TC and enrich TC using its porosity, thus enhancing the degradation efficiency of CBO. CBO@ZIF-8 showed good repeatability in both sensing and degradation process and demonstrated a great potential for wastewater multiple treatment.

In addition to TC, other antibiotics can also be treated by multifunctional MOFs. Wang and co-workers synthesized water-stable luminescent UiO-type MOFs (Zr-fcu-sti) for simultaneous sensing and removal of two nitrofurans (NFs) antibiotics (nitrofurazone, NZF and nitrofurantoin, NFT).[161] As shown in Fig. 14, the Zr-fcu-sti showed luminescence quenching toward the analyte and the detection limit was turned to be as low as 0.152 µM. The strong adsorption of nitrofurans at the excitation wavelength of Zr-fcu-sti, and the photo-induced electron transfer process from the organic ligand to nitrofurans are responsible for the sensing process. Interestingly, nitrofurans can lead to the bathochromic shift of the MOF's maximum emission, distinguishing them from other antibiotics, and this phenomenon can be used to detect nitrofurans qualitatively. As a result, Zr-fcu-sti showed a good selectivity while other antibiotics caused weaker luminescence quenching than nitrofurans. Moreover, the large surface area, proper pore size and the numerous hydrogen bonding sites in Zr-fcu-sti enabled such MOF to remove nitrofurans efficiently in water with the maximum adsorption capacity of 98 mg g^{-1} and 96 mg g^{-1} for nitrofurazone and nitrofurantoin, respectively. Zr-fcu-sti can be used as an effective material for monitoring and removal of nitrofurans in water.
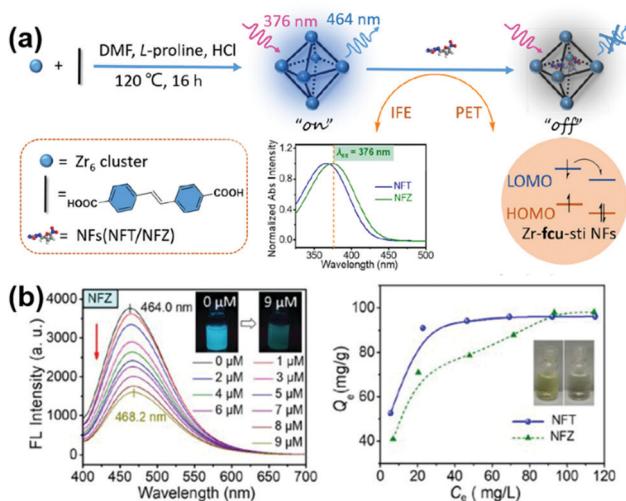
Fig. 14 (a) Schematic illustration of detection of NFs Based on Zr-fcu-sti and (b) sensing and removal of NFs on Zr-fcu-sti. Reproduced from ref. 161 with permission from Elsevier Inc, copyright 2022.

Ciprofloxacin is another typical antibiotic that is widely used in daily life. Basu's group constructed Fe–Cu binary MOF, MIL-53(Fe–Cu) through a single step solvothermal route to removal and degrade ciprofloxacin in water.[162] MIL-53(Fe–Cu) displayed beneficial properties such as porosity, high surface area, thermal stability, functional sites in framework and photocatalytic activity. The MOF showed a maximum adsorption capacity of 190.4 mg g^{-1} for ciprofloxacin. Molecular calculation was conducted to demonstrate the molecular level adsorption and a contact angle of 34.5° and a minimun bond-length of 4.3 Å were observed. For degradation, the maximum degradation of 74.48 and 57.88%, and a kinetic rate of 0.010 and 0.012 min^{-1} were obtained in the presence of UV and visible light, respectively. The photoluminescence (PL) spectra showed that MIL-53(Fe–Cu) offers a reduced rate of electron-hole recombination, which is benefit to the degradation procedure. In addition, the reusability made MIL-53(Fe–Cu) potential material in practical application.

Yang and co-workers designed two flexible 3D Zn-based MOFs, namely, ROD-Zn1 and ROD-Zn2 to sense and remove several antibiotics such as TC, nitrofurans (NZF and NFT) and chloramphenicols (chloramphenicol, CAP and thiamphenicol, THI).[163] The adsorption abilities on ROD-Zn1 and ROD-Zn2 follow a trend of TC > NZF > NFT > CAP > THI. The maximum adsorption capacities of TC on ROD-Zn1 and ROD-Zn2 were 142.9 and 125.0 mg g^{-1} and the adsorption can be finished with 40 min. As all the studied antibiotics can be adsorbed in the cavities of ROD-Zn MOFs, π–π interactions can occur between the analytes and MOFs. The different adsorption capacities may be ascribed to different electronic behaviors of antibiotics and TC with –NH$_2$ groups could generate hydrogen bonds with O–H on ligands of ROD-Zn MOFs, which may facilitate the adsorption process. ROD-Zn MOFs also displayed luminescence quenching towards the antibiotics, with the efficiencies followed the same order as in adsorption capacities. TC had quenching efficiencies of 96.4 and 95.1% on ROD-Zn1 and ROD-Zn2, respectively. ROD-Zn MOF had a good linear range of 0–45 µM towards TC with the detection limit of 0.11–0.12 µM. The experiment as well as DFT calculations revealed that Förster resonance energy transfer (FRET) and photoinduced electron transfer (PET) made these antibiotics show a diverse fluorescence quenching effect. Furthermore, the MOF-melamine foam (MF) hybrid was prepared via one-pot synthesis. The resulting microporous–macroporous MOF@MF demonstrated high mechanical stabilities, good recyclability and enhanced adsorption abilities, endowing such material with great potential in practical applications.

Besides antibiotics, other pharmaceuticals may also cause adverse effect to environment and human health, and are need to be treated. Yu and co-workers synthesized MIL-53(Fe) for remove and degrade two pharmaceuticals, viz., clofibric acid (CA) and carbamazepine (CBZ) from aqueous solution.[164] MIL-53(Fe) displayed good adsorption performance with the adsorption capacities of CA and CBZ of 0.80 and 0.57 mmol g^{-1}, respectively. The π–π interaction mainly contributed for the adsorption of CBZ, whereas electrostatic interactions are

responsible for the CA adsorption. Furthermore, the photocatalytic activity was studied. MIL-53(Fe) showed significantly improved photocatalytic efficiency up to 90% for both CA and CBZ with the addition of small amount of H_2O_2, and outperformed those of traditional catalysts such as $Fe(II)/H_2O_2$ and TiO_2 under visible light. Mechanism study revealed that upon irradiation, the charge carriers directly generated in MIL-53(Fe) and the synergistic effect of H_2O_2 accelerate the Fenton-like reaction. For practical application, MIL-53(Fe) was used for remove CA and CNZ in real municipal wastewater and river water, and exhibited good performance for wastewater treatment.

Expect that the metal/metal clusters can offer catalytic sites on MOFs, the organic ligand can also serve as a catalytic center for catalytic degradation. On this basis, Yu's group further explored a mixed-linker Zr-MOFs, PCN-134 to remove and degrade diclofenac (DF) in water.[165] As Zr-MOFs allows the partial absence of linkers without destroying the framework integrity. The defect extent can be controlled by different TCPP ligand ratios in PCN-134 and best ratio balancing the porosity and detects was achieved. As a result, defect PCN-134 showed a maximum adsorption capacity of 2.04 mmol g^{-1} towards DF. PCN-134 displayed good photocatalytic activity to DF under visible light with degradation efficiency of above 99% in 5 hours. As porphyrin unit can generate $^1O_2$, PCN-134 was dominated by type II photosensitization reaction, and the corresponding productivity was higher than that of single-linker PCN-224. Besides, the electron transformed between TCPP linker and Zr clusters also contributed to the photodegradation of DF. The enhanced behavior in PCN-224 mainly rely on the extra defect sites, open porous structure, synergistic effect between organic linkers and efficient energy transfer. Moreover, the good reusability and water stability made PCN-134 promising material for wastewater treatment.

3.2.4. EDCs treatment. The endocrine-disrupting chemicals can cause adverse effect on the endocrine systems of wildlife and human, bringing great threat to environment and human health.[166] As EDCs can be preconcentrated in human body and cause various diseases, *e.g.*, reproductive system damage and cancers, it is of great importance to detect and eliminate EDCs in aqueous environment.[167,168] phenolic compounds such as bisphenols are common EDCs and are in great demand in industry. Gu's group synthesized Zr-based porphyrin MOFs, PCN-222, for simultaneous removal and degradation of bisphenol A (BPA) from water.[169] The kinetic separation of adsorption and photodegradation process can be well controlled. PCN-222 showed an ultrahigh adsorption capacity of 487.7 mg g^{-1}, while the degradation process could be realized within 20 min at the rate of 0.004 mg min^{-1}. Interestingly, the research showed that the adsorption process had synergetic effect that promote the photocatalytic efficiency, as experiments confirmed that the catalysis happened inside the MOF pores instead of in the solution phase. Furthermore, various experiments were conducted to investigate the mechanism. The mechanism study showed that BPA was oxidized by the $^1O_2$ generated from porphyrin ligand within PCN-222 under

visible light. The excellent reusability with wide range pH suitability enabled such MOF for practical use.

Another example of porphyrin MOFs for phenolic compounds multiple treatment was presented by Gu's group (Fig. 15). In this work, a Zr-MOF, NU-1000 with mesopores was synthesized for removal and degradation of 4-chlorophenol (4-CP).[170] carboxylic β-cyclodextrin (CMCD) was incorporated into NUS-1000 to assist adsorbing 4-CP. 4-CP were inclined to form a stable inclusion complex with CMCD, which facilitate the adsorption process. As a result, a large adsorption capacity of 296 mg g^{-1} was obtained. The degradation experiments showed that CMCD@NU-1000 can detoxified 4-CP within 60 min, together with a half-life time of only 5.98 min under sunlight irradiation. The MOF containing porphyrin units could generate $^1O_2$ to oxidize the analyte under irradiation and played a vital role in the photodegradation of 4-CP through adsorption–degradation integrator. In addition, CMCD@NU-1000 can still keep 96% of its adsorption ability after five regeneration–adsorption cycles, indicating a good potential for practical use.

Enzymes have great potential in degrading pollutions as aforementioned. MOF–enzymes composites can also work on EDCs treatment. To this end, Wei and co-workers fabricated a laccase (LAC)-embedded MOF and its composite to sense and degrade phenolic pollutants.[171] To be specific, ZIF-90 was firstly encapsulated with LAC, and then combined with bacterial cellulose (BC) and carboxylated multi-walled carbon nanotubes to prepare a cellulose membrane. The MOF composite showed an electrochemical detection ability towards catechol. A linear range of 20-400 μM and a detection limit of 1.86 μM was acquired, together with satisfactory reproducibility and selectivity. Besides, the MOF–enzyme composite displayed higher degradation efficiency to catechol than pure LAC, as the porous ZIF-90 could increase the adsorption ability to catechol and protect the LAC from reducing the enzyme activity. The degradation efficiency of 93.4% was obtained and the MOF–enzyme membrane composite was successfully used in enzyme membrane reactor, holding a practical application prospect in the phenolic wastewater treatment.
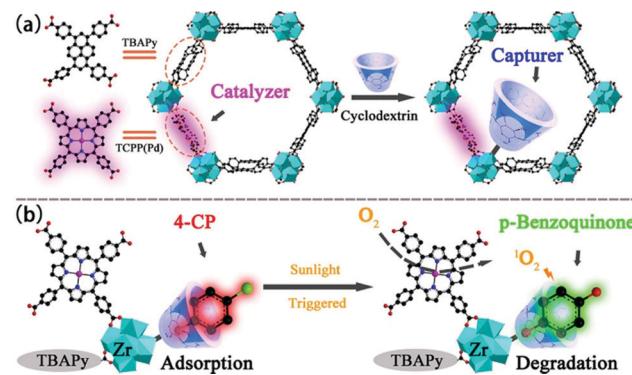

Fig. 15 (a) The construction of CMCD@NU-1000-TCPP(Pd) and (b) schematic illustration of the adsorption and degradation processes toward 4-CP. Reproduced from ref. 170 with permission from American Chemical Society, copyright 2021.

Table 1 Summary of MOFs for multiple treatment to water pollutions

Targets	MOF	Treatment model	Adsorption capacity	Limit of detection	DE[a] (%)	Ref.
Hg^{2+}	LMOF-263	R[b] & S[c]	380 mg g^{-1}	3.3 µg L^{-1}	—[f]	84
Hg^{2+}	NH$_2$-UiO66-SH	R & S	265.29 mg g^{-1}	0.035 µM	—	85
Hg^{2+}	NH$_2$-MIL-53(Al)	R & S	153.85 mg g^{-1}	0.15 µM	—	87
Hg^{2+}	TMU-46 ∼ 48S	R & S	714 mg g^{-1}	0.1 mg L^{-1}	—	88
Hg^{2+}	Ni-MOF	R & S	713 mg g^{-1}	Nm[e]	—	90
Hg^{2+}	Al-MOF monitors	R & S	1110 mg g^{-1}	0.8 µg L^{-1}	—	91
Hg^{2+}	Zr-DMBD MOFs	R & S	171.5 mg g^{-1}	0.05 µM	—	93
Cd^{2+}	FJI-H9	R & S	225 mg g^{-1}	10 mg L^{-1}	—	96
Cd^{2+}	Fe$_3$O$_4$/MOF/cysteine	R & S	248.2 mg g^{-1}	0.94 µg L^{-1}	—	100
Pb^{2+} & Cu^{2+}	NH$_2$-MIL-101(Fe)	R & S	0.9 and 1.1 mM g^{-1}	1.6–5.2 µM	—	101
UO_2^{2+}	Tb-MOF	R & S	179.08 mg g^{-1}	0.9 µg L^{-1}	—	106
Th^{4+}	ThP-1	R & S	25.82 mg g^{-1}	24.2 µg L^{-1}	—	107
IO_3^-	Th-MOF	R & S	152.6 mg g^{-1}	0.107 µg kg^{-1}	—	109
UO_2^{2+}	Fe$_3$O$_4$@ZIF-8@CDs	R & S	606.06 mg g^{-1}	Nm	—	110
$Cr_2O_7^{2-}$	BUT-39	R & S	215 mg g^{-1}	1.5 µM	—	113
$Cr_2O_7^{2-}$	Dyes⊂MOF-801	R & S	83 mg g^{-1}	30 µM	—	115
$Cr_2O_7^{2-}$	MOF-MMMs	R & S	33.34 mg g^{-1}	5.73 nM	—	117
$Cr_2O_7^{2-}$	UiO66-(OH)$_2$	R & D[d]	53.8 mg g^{-1}	—	Nm	120
$Cr_2O_7^{2-}$	Zr-MSA	R & D	202.0 mg g^{-1}	—	Nm	121
$Cr_2O_7^{2-}$	JLU-MOF60	R & S & D	149 mg g^{-1}	9.38 µM	98	122
F^-	NH$_2$-MIL-53(Al)	R & S	203 mg g^{-1}	0.31 µM	—	125
F^-	In-TCPP	R & S	36.7 mg g^{-1}	1.3 µg L^{-1}	—	126
AO7	Fe-based MOFs	R & D	31.4–153.4 mg g^{-1}	—	3.8–33.2	134
MB & MO	Fe loaded MOF-545(Fe)	R & D	382.4 and 803.7 mg g^{-1}	—	>99	135
MB & MO	Ni-doping MIL-101(Fe)	R & D	About 40 and 80 mg g^{-1}	—	>90	136
MB	MIL-53(Al-Fe)@SiO$_2$	R & D	681.78 mg g^{-1}	—	99.85	137
MB	Gold nanorods/MOFs	S & D	—	9.3 pM	60	138
RhB & MO	NH$_2$-MIL-101(Fe) membrane	R & D	Membrane 80–100% rejection	—	10–18	139
CV, MB, RhB	SCNU-Z2	R & D	455–847 mg g^{-1}	—	97	140
MB, MO, RhB and AO7	Ce-UiO-66	R & D	249–427 mg g^{-1}	—	81–99	141
RhB & MB	SNNU-110	R & D	51.6 mg g^{-1}	—	93.1–94.6	142
CR & RhB	Eu/Tb-MOF	R & D	Nm	—	>99	143
glyphosate	Fe$_3$O$_4$@SiO$_2$@UiO-67	R & S	256.54 mg g^{-1}	93 µg L^{-1}	—	147
Methyl parathion	OPH^{6His}@Tb-BTC	S & D	—	2.6 nM	82	152
TC	Eu-MOF	R & S	387 mg g^{-1}	3 nM	—	158
TC	Fe-MIL-MOF	R & D	Nm	—	96.6	159
TC	CBO@ZIF-8	S & D	—	26 nM	75.2	160
NZF & NFT	UiO-type MOF	R & S	96 and 98 mg g^{-1}	0.152 µM	—	161
CP	MIL-53(Fe–Cu)	R & D	190.4 mg g^{-1}	—	74.5	162
TC, CP, NFs and THI	ROD-Zn	R & S	142.9 mg g^{-1}	0.11–1.39 µM	—	163
CA & CBZ	MIL-53(Fe)	R & D	0.57 and 0.8 mmol g^{-1}	—	>90	164
DF	PCN-134	R & D	2.04 mmol g^{-1}	—	99	165
BPA	PCN-222	R & D	487 mg g^{-1}	—	99	169
4-CP	β-CD-NU-1000	R & D	296 mg g^{-1}	—	>90	170
Catechol	LAC-embedded MOF	S & D	—	1.86 µM	93.4	171

[a] Degradation efficiency. [b] Removal. [c] Sensing. [d] Degradation. [e] Not mentioned. [f] No function.

MOF and MOF composites have been reported to hold promising potential in organic water pollution treatment. The porosity, designability, tunability and functionality make MOFs ideal platform to realize more than one function of removal, sensing and degradation towards organic pollutions. Nevertheless, there is still space for improving sensing sensitivity, reusability and mechanism explanation. Table 1 lists the representative studies of MOFs for water pollution multiple treatment.

4. Conclusions and outlook

MOFs, as a shining star in porous coordination materials, have been widely exploited in various fields and drawn fascinating attention in the past decades. For water pollution treatment, realizing multiple function treatment towards one analyte simultaneously is of great convenience and might be the future trend. This feature article firstly discussed the importance of sensing, removal and degradation treatments towards water pollutions. Then, the attention was focused on MOFs, which displayed porosity, designability, stability and functionality, as an ideal platform to achieve multiple treatment to water pollutions. Afterwards, examples of MOFs/MOF composites for the multifunction treatment to inorganic/organic water pollution were summarized. Despite that MOFs possessed tremendous potential in wastewater treatment, some deficiencies may still restrain their further application. Hence, the challenges as well as opportunities should be thought about in the future as follows:

(1) The water stability of MOFs is still a problem. Although some typical MOFs showed stability in water, more MOFs tend

to decompose in aqueous system and acid/base solution, and the instability in water largely limits their practical applications. In fact, the MOFs for wastewater treatment as summarized above mainly centered on the UiO, MIL and ZIF serious typical MOFs that are stable in water. Considering the diversification of water pollutions, the current water stable MOFs are insufficient for the sensitive and selective treatment of various water pollutions, especially organic pollutions. Accordingly, enhancement in MOFs water stability is of vital importance in the future research. Exploiting water stable MOFs or fabricating MOF composites to improve their water resistance may be the possible ways.[172–176] Generally, improving the strength of the metal-ligand bond may help enhance the water resistance, for which HSAB offers a helpful guidance. To be specific, azolate-based ligands and low-valency transition metal ions, or carboxylate-based ligands and high-valency metal ions tend to form relative strong metal–ligand bond.[177] Besides, tuning the pore environments of MOFs, *e.g.*, constructing hydrophobic MOFs *via* delicate design to exclude the infusion of water is another conducive way to improve the water stability of MOFs.

(2) The deep understanding of structure–property relationship needs to improve. At present, how to choose MOFs for the treatment of a specific target lacks general guidance. Different water pollutions have varied size, hydrophilicity, polarity, electrical property and functional group, and there are a hundred thousand of MOFs with all kinds of topologies, pore size, center metal/metal clusters, connectivity and functional groups been explored. The current research of the analytes response on MOFs mostly relies on experiment screening, which may lead to huge amount of work and low efficiency. High-throughput computational screening may provide an optional plan.[178] As several databases have been established containing numerous MOFs structures, the required pores, binding sites or catalytic sites can be pre-programmed according to the property of the target molecules, and MOFs with potential interactions towards analytes can be screened out.

(3) The reusability needs more attention. Though many MOFs displayed regeneration and reusability, their removal and degradation performances usually decreased when the reuse cycles are above 3. During the recycle process, MOFs have the risk of leaking out into the water, and some MOFs containing toxic metals may cause second pollution in the environment. Thereby, to monitor the MOFs during the recycle process and to pay more attention to MOF reusability during design is necessary. Besides, the current research works usually investigate the reusability of MOFs with less than 10 cycles, and long-term efficiency of MOFs for water treatment need to be further explored, ensuring MOFs as a long-tested material for practical application.

(4) The mechanisms of MOFs for water pollution multiple treatment should be investigated more deeply. Many works discussed the removal, sensing and degradation mechanisms by experiment measurement or computational calculations, and explained the behavior to some extent. However, MOFs have the unique advantages compared with covalent organic frameworks or other porous materials as MOFs can obtain single crystal form, which is effective for revealing the mechanisms. Therefore, if the crystal form of MOF-analyte combinations is acquired, there will be convincing evidence to illustrate the mechanisms.

Although there are still challenges to exploit the MOFs as multifunctional materials in wastewater treatment, it is undeniable that the exploration of MOFs brings more promising thoughts to the researchers. They will keep devoting themselves to designing and constructing suitable MOFs and multifunctional MOFs for wastewater treatment will have a bright future.

Conflicts of interest

There are no conflicts to declare.

Acknowledgements

Notes and references

1 F. G. Acién, C. Gómez-Serrano, M. M. Morales-Amaral, J. M. Fernández-Sevilla and E. Molina-Grima, *Appl. Microbiol. Biotechnol.*, 2016, **100**, 9013–9022.
2 S. Bolisetty, M. Peydayesh and R. Mezzenga, *Chem. Soc. Rev.*, 2019, **48**, 463–487.
3 J. Li, X. X. Wang, G. X. Zhao, C. L. Chen, Z. F. Chai, A. Alsaedi, T. Hayat and X. K. Wang, *Chem. Soc. Rev.*, 2018, **47**, 2322–2356.
4 D. Banerjee, D. Kim, M. J. Schweiger, A. A. Kruger and P. K. Thallapally, *Chem. Soc. Rev.*, 2016, **45**, 2724–2739.
5 M. Nasiri, H. Ahmadzadeh and A. Amiri, *TrAC, Trends Anal. Chem.*, 2020, **123**, 115772.
6 K. H. Chu, Y. A. J. Al-Hamadani, C. M. Park, G. Lee, M. Jang, A. Jang, N. Her, A. Son and Y. Yoon, *Chem. Eng. J.*, 2017, **327**, 629–647.
7 M. Lorenzo, J. Campo and Y. Picó, *TrAC, Trends Anal. Chem.*, 2018, **103**, 137–155.
8 S. Rojas and P. Horcajada, *Chem. Rev.*, 2020, **120**, 8378–8415.
9 Y. H. Pi, X. Y. Li, Q. B. Xia, J. L. Wu, Y. W. Li, J. Xiao and Z. Li, *Chem. Eng. J.*, 2018, **337**, 351–371.
10 R. Das, C. D. Vecits, A. Schulze, B. Cao, A. F. Ismail, X. Lu, J. Chen and S. Ramakrishna, *Chem. Soc. Rev.*, 2017, **46**, 6946–7020.
11 M. Patel, R. Kumar, K. Kishor, T. Mlsna, C. U. Pittman and D. Mohan, *Chem. Rev.*, 2019, **119**, 3510–3673.
12 S. Mao, J. Chang, G. Zhou and J. Chen, *Small*, 2015, **11**, 5336–5359.
13 D. Dai, J. Yang, Y. Wang and Y. W. Yang, *Adv. Funct. Mater.*, 2021, **31**, 2006168.
14 B. Bansod, T. Kumar, R. Thakur, S. Rana and I. Singh, *Biosens. Bioelectron.*, 2017, **94**, 443–455.
15 S. Y. Chen, Z. Li, K. Li and X. Q. Yu, *Coord. Chem. Rev.*, 2021, **429**, 213691.
16 B. O. Okesola and D. K. Smith, *Chem. Soc. Rev.*, 2016, **45**, 4226–4251.
17 M. Gao, G. Liu, Y. Gao, G. Chen, X. Huang, X. Xu, J. Wang, X. Yang and D. Xu, *TrAC, Trends Anal. Chem.*, 2021, **137**, 116226.
18 C. Jung, J. Oh and Y. Yoon, *Environ. Sci. Pollut. Res.*, 2015, **22**, 10058–10069.
19 F. Dixit, R. Dutta, B. Barbeau, P. Berube and M. Mohseni, *Chemosphere*, 2021, **272**, 129777.
20 J. Völker, M. Stapf, U. Miehe and M. Wagner, *Environ. Sci. Technol.*, 2019, **53**, 7215–7233.

21 N. Jiang, R. Shang, S. G. J. Heijman and L. C. Rietveld, *Water Res.*, 2018, **144**, 145–161.

22 M. K. Uddin, *Chem. Eng. J.*, 2017, **308**, 438–462.

23 P. L. Yap, M. J. Nine, K. Hassan, T. T. Tung, D. N. H. Tran and D. Losic, *Adv. Funct. Mater.*, 2021, **31**, 2007356.

24 T. H. Boyer, Y. Fang, A. Ellis, R. Dietz, Y. J. Choi, C. E. Schaefer, C. P. Higgins and T. J. Strathmann, *Water Res.*, 2021, **200**, 117244.

25 F. Yu, X. Bai, M. Liang and J. Ma, *Chem. Eng. J.*, 2021, **405**, 126960.

26 Y. Zhu, W. Fan, W. Feng, Y. Wang, S. Liu, Z. Dong and X. Li, *J. Hazard. Mater.*, 2021, **414**, 125517.

27 J. Wang and Z. Bai, *Chem. Eng. J.*, 2017, **312**, 79–98.

28 S. W. Nam, Y. Yoon, D. J. Choi and K. D. Zoh, *J. Hazard. Mater.*, 2015, **285**, 453–463.

29 V. Choudhary, K. Vellingiri, M. I. Thayyil and L. Philip, *Environ. Sci.: Nano*, 2021, **8**, 1133–1176.

30 S. Wu, Y. Lin and Y. H. Hu, *J. Mater. Chem. A*, 2021, **9**, 2592–2611.

31 M. Pedrosa, J. L. Figueiredo and A. M. T. Silva, *J. Environ. Chem. Eng.*, 2021, **9**, 104930.

32 H. Sun, C. Kwan, A. Suvorova, H. M. Ang, M. O. Tadé and S. Wang, *Appl. Catal., B*, 2014, **154–155**, 134–141.

33 X. Liu, R. Ma, L. Zhuang, B. Hu, J. Chen, X. Liu and X. K. Wang, *Crit. Rev. Environ. Sci. Technol.*, 2021, **51**, 751–790.

34 V. K. Sharma and M. Feng, *J. Hazard. Mater.*, 2019, **372**, 3–16.

35 Y. Zhou, L. Tang, G. Zeng, J. Chen, Y. Cai, Y. Zhang, G. Yang, Y. Liu, C. Zhang and W. Tang, *Biosens. Bioelectron.*, 2014, **61**, 519–525.

36 H. Dong, G. Zeng, L. Tang, C. Fan, C. Zhang, X. He and Y. He, *Water Res.*, 2015, **79**, 128–146.

37 Q. Hua, J. Sun, H. Liu, R. Bao, R. Yu, J. Zhai, C. Pan and Z. L. Wang, *Nat. Commun.*, 2018, **9**, 244.

38 J. N. Tiwari, S. Sultan, C. W. Myung, T. Yoon, N. Li, M. Ha, A. M. Harzandi, H. J. Park, D. Y. Kim, S. S. Chandrasekaran, W. G. Lee, V. Vij, H. Kang, T. J. Shin, H. S. Shin, G. Lee, Z. Lee and K. S. Kim, *Nat. Energy*, 2018, **3**, 773–782.

39 P. Cheng and K. Pu, *Nat. Rev. Mater.*, 2021, **6**, 1095–1113.

40 H. Li, M. Eddaoudi, M. O'Keeffe and O. M. Yaghi, *Nature*, 1999, **402**, 276–279.

41 X. Zhao, Y. Wang, D. S. Li, X. Bu and P. Feng, *Adv. Mater.*, 2018, **30**, 1705189.

42 H. Y. Li, S. N. Zhao, S. Q. Zhang and J. Li, *Chem. Soc. Rev.*, 2020, **49**, 6364–6401.

43 X. Liu, T. Yue, K. Qi, Y. Qiu, B. Y. Xia and X. Guo, *Chin. Chem. Lett.*, 2020, **31**, 2189–2201.

44 Y. Du, X. Gao, S. Li, L. Wang and B. Wang, *Chin. Chem. Lett.*, 2020, **31**, 609–616.

45 G. R. Xu, Z. H. An, K. Xu, Q. Liu, R. Das and H. L. Zhao, *Coord. Chem. Rev.*, 2021, **427**, 213554.

46 V. Kumar, V. Singh, K. H. Kim, E. E. Kwon and S. A. Younis, *Coord. Chem. Rev.*, 2021, **447**, 214148.

47 R. J. Drout, L. Robison, Z. Chen, T. Islamoglu and O. K. Farha, *Trends Chem.*, 2019, **1**, 304–317.

48 Y. Xiao, Y. Cui, Q. Zheng, S. Xiang, G. Qian and B. Chen, *Chem. Commun.*, 2010, **46**, 5503–5505.

49 M. Alvaro, E. Carbonell, B. Ferrer, F. X. Llabrés i Xamena and H. Garcia, *Chem. – Eur. J.*, 2007, **13**, 5106–5112.

50 E. Haque, J. E. Lee, I. T. Jang, Y. K. Hwang, J. S. Chang, J. Jegal and S. H. Jhung, *J. Hazard. Mater.*, 2010, **181**, 535–542.

51 Z. Chen, K. O. Kirlikovali, P. Li and O. K. Farha, *Acc. Chem. Res.*, 2022, **55**, 579–591.

52 C. C. Wang, J. R. Li, X. L. Lv, Y. Q. Zhang and G. Guo, *Energy Environ. Sci.*, 2014, **7**, 2831–2867.

53 A. Karmakar, P. Samanta, A. V. Desai and S. K. Ghosh, *Acc. Chem. Res.*, 2017, **50**, 2457–2469.

54 Z. Hasan and S. H. Jhung, *J. Hazard. Mater.*, 2015, **283**, 329–339.

55 C. Wang, X. Liu, N. K. Demir, J. P. Chen and K. Li, *Chem. Soc. Rev.*, 2016, **45**, 5107–5134.

56 J. Liu, C. Chen, K. Zhang and L. Zhang, *Chin. Chem. Lett.*, 2021, **32**, 649–659.

57 P. Samanta, A. V. Desai, S. Sharma, P. Chandra and S. K. Ghosh, *Inorg. Chem.*, 2018, **57**, 2360–2364.

58 W. P. Lustig, S. Mukherjee, N. D. Rudd, A. V. Desai, J. Li and S. K. Ghosh, *Chem. Soc. Rev.*, 2017, **46**, 3242–3285.

59 J. Jin, J. Xue, Y. Liu, G. Yang and Y. Y. Wang, *Dalton Trans.*, 2021, **50**, 1950–1972.

60 S. Li, Y. Li and B. Yan, *CrystEngComm*, 2021, **23**, 5345–5352.

61 X. Fang, B. Zong and S. Mao, *Nano-Micro Lett.*, 2018, **10**, 64.

62 W. Lu, Z. Wei, Z. Y. Gu, T. F. Liu, J. Park, J. Park, J. Tian, M. Zhang, Q. Zhang, T. Gentle, M. Bosch and H. C. Zhou, *Chem. Soc. Rev.*, 2014, **43**, 5561–5593.

63 C. Negro, H. Martínez, P. Cejuela, E. F. Simó-Alfonso, J. M. Herrero-Martínez, R. Bruno, D. Armentano, J. Ferrando-Soria and E. Pardo, *ACS Appl. Mater. Interfaces*, 2021, **13**, 28424–28432.

64 Y. Chen, B. Wang, X. Wang, L. H. Xie, J. Li, Y. Xie and J. R. Li, *ACS Appl. Mater. Interfaces*, 2017, **9**, 27027–27035.

65 Y. Li, G. Hou, J. Yang, J. Xie, X. Yuan, H. Yang and M. Wang, *RSC Adv.*, 2016, **6**, 16395–16403.

66 Q. Li, D. X. Xue, Y. F. Zhang, Z. H. Zhang, Z. Gao and J. Bai, *J. Mater. Chem. A*, 2017, **5**, 14182–14189.

67 C. Zhou, C. Lai, D. Huang, G. Zeng, C. Zhang, M. Cheng, L. Hu, J. Wan, W. Xiong, M. Wen, X. Wen and L. Qin, *Appl. Catal., B*, 2018, **220**, 202–210.

68 E. Flage-Larsen, A. Røyset, J. H. Cavka and K. Thorshaug, *J. Phys. Chem. C*, 2013, **117**, 20610–20616.

69 R. Liang, F. Jing, L. Shen, N. Qin and L. Wu, *Nano Res.*, 2015, **8**, 3237–3249.

70 R. Liang, S. Luo, F. Jing, L. Shen, N. Qin and L. Wu, *Appl. Catal., B*, 2015, **176-177**, 240–248.

71 T. Zeng, D. Shi, Q. Cheng, G. Liao, H. Zhou and Z. Pan, *Environ. Sci.: Nano*, 2020, **7**, 861–879.

72 X. Wang, J. Liu, S. Leong, X. Lin, J. Wei, B. Kong, Y. Xu, Z. X. Low, J. Yao and H. Wang, *ACS Appl. Mater. Interfaces*, 2016, **8**, 9080–9087.

73 M. A. Ahsan, V. Jabbari, M. A. Imam, E. Castro, H. Kim, M. L. Curry, D. J. Valles-Rosales and J. C. Noveron, *Sci. Total Environ.*, 2020, **698**, 134214.

74 W. Huang, N. Liu, X. Zhang, M. Wu and L. Tang, *Appl. Surf. Sci.*, 2017, **425**, 107–116.

75 X. S. Miao, F. Bishay, M. Chen and C. D. Metcalfe, *Environ. Sci. Technol.*, 2004, **38**, 3533–3541.

76 Y. Luo, W. Guo, H. H. Ngo, L. D. Nghiem, F. I. Hai, J. Zhang, S. Liang and X. C. Wang, *Sci. Total Environ.*, 2014, **473-474**, 619–641.

77 F. Murphy, C. Ewins, F. Carbonnier and B. Quinn, *Environ. Sci. Technol.*, 2016, **50**, 5800–5808.

78 J. A. Camargo and Á. Alonso, *Environ. Int.*, 2006, **32**, 831–849.

79 S. Dutta, S. Let, S. Sharma, D. Mahato and S. K. Ghosh, *Chem. Rec.*, 2021, **21**, 1666–1680.

80 N. Sharma, A. K. Dey, R. Y. Sathe, A. Kumar, V. Krishnan, T. J. D. Kumar and C. M. Nagaraja, *Catal. Sci. Technol.*, 2020, **10**, 7724–7733.

81 M. E. Mahmoud, S. M. Elsayed, S. E. M. E. Mahmoud, R. O. Aljedaani and M. A. Salam, *J. Mol. Liq.*, 2022, **347**, 118274.

82 F. Zahir, S. J. Rizwi, S. K. Haq and R. H. Khan, *Environ. Toxicol. Pharmacol.*, 2005, **20**, 351–360.

83 L. D. Hylander and M. E. Goodsite, *Sci. Total Environ.*, 2006, **368**, 352–370.

84 N. D. Rudd, H. Wang, E. M. A. Fuentes-Fernandez, S. J. Teat, F. Chen, G. Hall, Y. J. Chabal and J. Li, *ACS Appl. Mater. Interfaces*, 2016, **8**, 30294–30303.

85 T. Li, Mark T. Kozlowski, E. A. Doud, M. N. Blakely and N. L. Rosi, *J. Am. Chem. Soc.*, 2013, **135**, 11688–11691.

86 L. Zhang, J. Wang, H. Wang, W. Zhang, W. Zhu, T. Du, Y. Ni, X. Xie, J. Sun and J. Wang, *Nano Res.*, 2021, **14**, 1523–1532.

87 L. Zhang, J. Wang, T. Du, W. Zhang, W. Zhu, C. Yang, T. Yue, J. Sun, T. Li and J. Wang, *Inorg. Chem.*, 2019, **58**, 12573–12581.

88 L. Esrafili, M. Gharib and A. Morsali, *New J. Chem.*, 2019, **43**, 18079–18091.

89 G. Chen, Z. Guo, G. Zeng and L. Tang, *Analyst*, 2015, **140**, 5400–5443.

90 S. Halder, J. Mondal, J. Ortega-Castro, A. Frontera and P. Roy, *Dalton Trans.*, 2017, **46**, 1943–1950.

91 A. Radwan, I. M. El-Sewify, A. Shahat, H. M. E. Azzazy, M. M. H. Khalil and M. F. El-Shahat, *ACS Sustainable Chem. Eng.*, 2020, **8**, 15097–15107.

92 Y. Zhang, G. M. Zeng, L. Tang, J. Chen, Y. Zhu, X. X. He and Y. He, *Anal. Chem.*, 2015, **87**, 989–996.

93 H. Yang, C. Peng, J. Han, Y. Song and L. Wang, *Sens. Actuators, B*, 2020, **320**, 128447.

94 P. A. Kobielska, A. J. Howarth, O. K. Farha and S. Nayak, *Coord. Chem. Rev.*, 2018, **358**, 92–107.

95 N. Lubick and D. Malakoff, *Science*, 2013, **341**, 1443.
96 H. Xue, Q. Chen, F. Jiang, D. Yuan, G. Lv, L. Liang, L. Liu and M. Hong, *Chem. Sci.*, 2016, **7**, 5983–5988.
97 Y. Wang, G. Ye, H. Chen, X. Hu, Z. Niu and S. Ma, *J. Mater. Chem. A*, 2015, **3**, 15292–15298.
98 Q. R. Fang, D. Q. Yuan, J. Sculley, J. R. Li, Z. B. Han and H. C. Zhou, *Inorg. Chem.*, 2010, **49**, 11637.
99 B. E. Meteku, J. Huang, J. Zeng, F. Subhan, F. Feng, Y. Zhang, Z. Qiu, S. Aslam, G. Li and Z. Yan, *Coord. Chem. Rev.*, 2020, **413**, 213261.
100 L. Fan, M. Deng, C. Lin, C. Xu, Y. Liu, Z. Shi, Y. Wang, Z. Xu, L. Li and M. He, *RSC Adv.*, 2018, **8**, 10561–10572.
101 S. W. Lv, J. M. Liu, C. Y. Li, N. Zhao, Z. H. Wang and S. Wang, *Chem. Eng. J.*, 2019, **375**, 122111.
102 X. Zhang and Y. Liu, *Environ. Sci.: Nano*, 2020, **7**, 1008–1040.
103 K. Jin, B. Lee and J. Park, *Coord. Chem. Rev.*, 2020, **427**, 213473.
104 S. Rapti, S. A. Diamantis, A. Dafnomili, A. Pournara, E. Skliri, G. S. Armatas, A. C. Tsipis, I. Spanopoulos, C. D. Malliakas, M. G. Kanatzidis, J. C. Plakatouras, F. Noli, T. Lazarides and M. J. Manos, *J. Mater. Chem. A*, 2018, **6**, 20813–20821.
105 S. Khan and S. K. Mandal, *ACS Appl. Mater. Interfaces*, 2021, **13**, 45465–45474.
106 W. Liu, X. Dai, Z. Bai, Y. Wang, Z. Yang, L. Zhang, L. Xu, L. Chen, Y. Li, D. Gui, J. Diwu, J. Wang, R. Zhou, Z. Chai and S. Wang, *Environ. Sci. Technol.*, 2017, **51**, 3911–3921.
107 W. Liu, X. Dai, Y. Wang, L. Song, L. Zhang, D. Zhang, J. Xie, L. Chen, J. Diwu, J. Wang, Z. Chai and S. Wang, *Environ. Sci. Technol.*, 2019, **53**, 332–341.
108 M. I. Gonzalez, A. B. Turkiewicz, L. E. Darago, J. Oktawiec, K. Bustillo, F. Grandjean, G. J. Long and J. R. Long, *Nature*, 2019, **577**, 64.
109 Z. J. Li, M. Lei, H. Bao, Y. Ju, H. Lu, Y. Li, Z. H. Zhang, X. Guo, Y. Qian, M. Y. He, J. Q. Wang, W. Liu and J. Lin, *Chem. Sci.*, 2021, **12**, 15833–15842.
110 X. Guo, Q. Liu, J. Liu, H. Zhang, J. Yu, R. Chen, D. Song, R. Li and J. Wang, *Appl. Surf. Sci.*, 2019, **491**, 640–649.
111 S. Prasad, K. K. Yadav, S. Kumar, N. Gupta, M. M. S. Cabral-pinto, S. Rezania, N. Radwan and J. Alam, *J. Environ. Manage.*, 2021, **285**, 112174.
112 C. E. Barrera-Díaz, V. Lugo-Lugo and B. Bilyeu, *J. Hazard. Mater.*, 2012, **223–224**, 1–12.
113 T. He, Y. Z. Zhang, X. J. Kong, J. Yu, X. L. Lv, Y. Wu, Z. J. Guo and J. R. Li, *ACS Appl. Mater. Interfaces*, 2018, **10**, 16650–16659.
114 S. H. Park, N. Kwon, J. H. Lee, J. Yoon and I. Shin, *Chem. Soc. Rev.*, 2020, **49**, 143–179.
115 J. Yoo, U. Ryu, W. Kwon and K. M. Choi, *Sens. Actuators, B*, 2019, **283**, 426–433.
116 S. Yu, H. Pang, S. Huang, H. Tang, S. Wang, M. Qiu, Z. Chen, H. Yang, G. Song, D. Fu, B. Hu and X. Wang, *Sci. Total Environ.*, 2021, **800**, 149662.
117 S. Zhang, H. Zheng, Y. Yang, G. Qian and Y. Cui, *Front. Chem.*, 2022, **10**, 852402.
118 H. P. Singh, P. M. S. Kaur, D. R. Batish and R. K. Kohli, *Environ. Chem. Lett.*, 2013, **11**, 229–254.
119 C. C. Wang, X. D. Du, J. Li, X. X. Guo, P. Wang and J. Zhang, *Appl. Catal., B*, 2016, **193**, 198–216.
120 Z. Wang, J. Yang, Y. Li, Q. Zhuang and J. Gu, *Chem. – Eur. J.*, 2017, **23**, 15415–15423.
121 P. Yang, Y. Shu, Q. Zhuang, Y. Li and J. Gu, *Langmuir*, 2019, **35**, 16226–16233.
122 J. Liu, Y. Ye, X. Sun, B. Liu, G. Li, Z. Liang and Y. Liu, *J. Mater. Chem. A*, 2019, **7**, 16833–16841.
123 X. Yang, Q. Zheng, M. He, B. Chen and B. Hu, *Water Res.*, 2021, **202**, 117401.
124 Y. Zhou, J. F. Zhang and J. Yoon, *Chem. Rev.*, 2014, **114**, 5511–5571.
125 D. H. Xie, X. Ge, W. X. Qin and Y. X. Zhang, *Chin. J. Chem. Phys.*, 2021, **34**, 227.
126 H. Q. Yin, K. Tan, S. Jensen, S. J. Teat, S. Ullah, X. Hei, E. Velasco, K. Oyekan, N. Meyer, X. Y. Wang, T. Thonhauser, X. B. Yin and J. Li, *Chem. Sci.*, 2021, **12**, 14189–14197.
127 L. Joseph, B. M. Jun, M. Jang, C. M. Park, J. C. Muñoz-Senmache, A. J. Hernández-Maldonado, A. Heyden, M. Yu and Y. Yoon, *Chem. Eng. J.*, 2019, **369**, 928–946.
128 D. J. Lapworth, N. Baran, M. E. Stuart and R. S. Ward, *Environ. Pollut.*, 2012, **163**, 287–303.
129 S. Dhaka, R. Kumar, A. Deep, M. B. Kurade, S. W. Ji and B. H. Jeon, *Coord. Chem. Rev.*, 2019, **380**, 330–352.
130 J. B. DeCoste and G. W. Peterson, *Chem. Rev.*, 2014, **114**, 5695–5727.
131 B. O. Okesola and D. K. Smith, *Chem. Soc. Rev.*, 2016, **45**, 4226–4251.
132 Y. Liu, Y. Zhao and J. Wang, *J. Hazard. Mater.*, 2021, **404**, 124191.
133 M. Cheng, C. Lai, Y. Liu, G. Zeng, D. Huang, C. Zhang, L. Qin, L. Hu, C. Zhou and W. Xiong, *Coord. Chem. Rev.*, 2018, **368**, 80–92.
134 X. Li, W. Guo, Z. Liu, R. Wang and H. Liu, *Appl. Surf. Sci.*, 2016, **369**, 130–136.
135 C. Zhang, H. Li, C. Li and Z. Li, *Molecules*, 2020, **25**, 168.
136 Q. Wu, M. S. Siddique and W. Yu, *J. Hazard. Mater.*, 2021, **401**, 123261.
137 A. Chatterjee, A. K. Jana and J. K. Basu, *Mater. Res. Bull.*, 2021, **138**, 111227.
138 X. Zhao, T. Yang, D. Wang, N. Zhang, H. Yang, X. Jing, R. Niu, Z. Yang, Y. Xie and L. Meng, *Anal. Chem.*, 2022, **94**, 4484–4494.
139 K. Vinothkumar, M. S. Jyothi, C. Lavanya, M. Sakar, S. Valiyaveettil and R. G. Balakrishna, *Chem. Eng. J.*, 2022, **428**, 132561.
140 S. Q. Deng, Y. L. Miao, Y. L. Tan, H. N. Fang, Y. T. Li, X. J. Mo, S. L. Cai, J. Fan, W. G. Zhang and S. R. Zheng, *Inorg. Chem.*, 2019, **58**, 13979–13987.
141 D. Zhao and C. Cai, *Dyes Pigm.*, 2021, **185**, 108957.
142 H. P. Li, Z. Dou, S. Q. Chen, M. Hu, S. Li, H. M. Sun, Y. Jiang and Q. G. Zhai, *Inorg. Chem.*, 2019, **58**, 11220–11230.
143 M. T. Hang, Y. Chen, Y. T. Wang, H. Li, M. Q. Zheng, M. Y. He, Q. Chen and Z. H. Zhang, *CrystEngComm*, 2022, **24**, 552–559.
144 F. H. M. Tang, M. Lenzen, A. McBratney and F. Maggi, *Nat. Geosci.*, 2021, **14**, 206–210.
145 M. Syafrudin, R. A. Kristanti, A. Yuniarto, T. Hadibarata, J. Rhee, W. A. Al-onazi, T. S. Algarni, A. H. Alwarri and A. M. Al-Mohaimeed, *Int. J. Environ. Res. Public Health*, 2021, **18**, 468.
146 G. Aragay, F. Pino and A. Merkçi, *Chem. Rev.*, 2012, **112**, 5317–5338.
147 Q. Yang, J. Wang, X. Chen, W. Yang, H. Pei, N. Hu, Z. Li, Y. Suo, T. Li and J. Wang, *J. Mater. Chem. A*, 2018, **6**, 2184–2192.
148 L. F. Stadlmair, T. Letzel, J. E. Drewes and J. Grassmann, *Chemosphere*, 2018, **205**, 649–661.
149 M. Wang, S. K. Mohanty and S. Mahendra, *Acc. Chem. Res.*, 2019, **52**, 876–885.
150 W. Liang, P. Wied, F. Carraro, C. J. Sumby, B. Nidetzky, C. K. Tsung, P. Falcaro and C. J. Doonan, *Chem. Rev.*, 2021, **121**, 1077–1129.
151 X. Lian, Y. Fang, E. Joseph, Q. Wang, J. Li, S. Banerjee, C. Lollar, X. Wang and H. C. Zhou, *Chem. Soc. Rev.*, 2017, **46**, 3386–3401.
152 J. Mehta, S. Dhaka, N. Bhardwaj, A. K. Paul, S. Dayananda, S. E. Lee, K. H. Kim and A. Deep, *Sens. Actuators, B*, 2019, **290**, 267–274.
153 T. A. Ternes, A. Joss and H. Siegrist, *Environ. Sci. Technol.*, 2004, **38**, 392A–399A.
154 Y. Yang, S. Ok, K. H. Kim, E. E. Kwon and Y. F. Tsang, *Sci. Total Environ.*, 2017, **596–597**, 303–320.
155 Y. Xu, T. Liu, Y. Zhang, F. Ge, R. M. Steel and L. Sun, *J. Mater. Chem. A*, 2017, **5**, 12001–12014.
156 E. Jin, S. Lee, E. Kang, Y. Kim and W. Choe, *Coord. Chem. Rev.*, 2020, **425**, 213526.
157 F. Wang, F. Ren, P. Mu, Z. Zhu, H. Sun, C. Ma, C. Xiao, W. Liang, L. Chen and A. Li, *J. Mater. Chem. A*, 2017, **5**, 11348–11356.
158 Y. Zhao, Q. Wang, H. Wang, H. Zhangsun, X. Sun, T. Bu, Y. Liu, W. Wang, Z. Xu and L. Wang, *Sens. Actuators, B*, 2021, **334**, 129610.
159 D. Wang, F. Jia, H. Wang, F. Chen, Y. Fang, W. Dong, G. Zeng, X. Li, Q. Yang and X. Yuan, *J. Colloid Interface Sci.*, 2018, **519**, 273–284.
160 Y. Gao, J. Wu, J. Wang, Y. Fan, S. Zhang and W. Dai, *ACS Appl. Mater. Interfaces*, 2020, **12**, 11036–11044.
161 P. Su, A. Zhang, L. Yu, H. Ge, N. Wang, S. Huang, Y. Ai, X. Wang and S. Wang, *Sens. Actuators, B*, 2022, **350**, 130865.
162 A. Chatterjee, A. K. Jana and J. K. Basu, *New J. Chem.*, 2021, **45**, 17196–17210.
163 S. Gai, J. Zhang, R. Fan, K. Xing, W. Chen, K. Zhu, X. Zheng, P. Wang, X. Fang and Y. Yang, *ACS Appl. Mater. Interfaces*, 2020, **12**, 8650–8662.
164 Y. Gao, G. Yu, K. Liu, S. Deng, B. Wang, J. Huang and Y. Wang, *Chem. Eng. J.*, 2017, **330**, 157–165.
165 Y. Gao, J. Xia, D. Liu, R. Kang, G. Yu and S. Deng, *Chem. Eng. J.*, 2019, **378**, 122118.

166 L. G. Kahn, C. Philippat, S. F. Nakayama, R. Slama and L. Trasande, *Lancet Diabetes Endocrinol.*, 2020, **8**, 703–718.

167 M. A. La Merrill, L. N. Vandenberg, M. T. Smith, W. Goodson, P. Browne, H. B. Patisaul, K. Z. Guyton, A. Kortenkamp, V. J. Cogliano, T. J. Woodruff, L. Rieswijk, H. Sone, K. S. Korach, A. C. Gore, L. Zeise and R. T. Zoeller, *Nat. Rev. Endocrinol.*, 2020, **16**, 45–57.

168 A. C. Gore, V. A. Chappell, S. E. Fenton, J. A. Flaws, A. Nadal, G. S. Prins, J. Toppari and R. T. Zoeller, *Endocr. Rev.*, 2015, **36**, 1–150.

169 A. N. Meng, L. X. Chaihu, H. H. Chen and Z. Y. Gu, *Sci. Rep.*, 2017, **7**, 6297.

170 W. Zhang, M. Gong, J. Yang and J. Gu, *Langmuir*, 2021, **37**, 8157–8166.

171 D. Li, Y. Cheng, H. Zuo, W. Zhang, G. Pan, Y. Fu and Q. Wei, *J. Colloid Interface Sci.*, 2021, **603**, 771–782.

172 Y. Zhao, R. L. Wang, X. X. Wu and C. D. Yang, *Chin. J. Struct. Chem.*, 2019, **38**, 991–998.

173 X. Qian, S. Deng, X. Chen, Q. Gao, Y. L. Hou, A. Wang and L. Chen, *Chin. Chem. Lett.*, 2020, **31**, 2211–2214.

174 L. Zhang, X. Y. Wu, C. Z. Lu and W. Z. Chen, *Chin. J. Struct. Chem.*, 2016, **35**, 1929–1935.

175 R. Wang, X. Y. Dong, H. Xu, R. B. Pei, M. L. Ma, S. Q. Zang, H. W. Hou and T. C. W. Mak, *Chem. Commun.*, 2014, **50**, 9153–9156.

176 Z. W. Zhai, S. H. Yang, M. Cao, L. K. Li, C. X. Du and S. Q. Zang, *Cryst. Growth Des.*, 2018, **18**, 7173–7182.

177 S. Yuan, L. Feng, K. Wang, J. Pang, M. Bosch, C. Lollar, Y. Sun, J. Qin, X. Yang, P. Zhang, Q. Wang, L. Zou, Y. Zhang, L. Zhang, Y. Fang, J. Li and H. C. Zhou, *Adv. Mater.*, 2018, **30**, 1704303.

178 Y. J. Colón and R. Q. Snurr, *Chem. Soc. Rev.*, 2014, **43**, 5735–5749.